Gao *et al. Microstructures* **2025**, *5*, 2025018
DOI: 10.20517/microstructures.2024.47

Microstructures

Review

Open Access

Check for updates

Recent progresses of non-oxide manganese and vanadium cathode materials for aqueous zinc ion batteries

Wujie Gao[1], Jiayue Feng[1], Shuaipeng Wang[1], Tingsheng Wang[1], Songcan Wang[1,2]

[1]Frontiers Science Center for Flexible Electronics, Xi'an Institute of Flexible Electronics (IFE), Northwestern Polytechnical University, Xi'an 710072, Shaanxi, China.
[2]Key Laboratory of Flexible Electronics of Zhejiang Province, Ningbo Institute of Northwestern Polytechnical University, Ningbo 315103, Zhejiang, China.

Correspondence to: Dr. Songcan Wang, Frontiers Science Center for Flexible Electronics, Xi'an Institute of Flexible Electronics (IFE), Northwestern Polytechnical University, 127 West Youyi Road, Xi'an 710072, Shaanxi, China. E-mail: iamscwang@nwpu.edu.cn

How to cite this article: Gao, W.; Feng, J.; Wang, S.; Wang, T.; Wang, S. Recent progresses of non-oxide manganese and vanadium cathode materials for aqueous zinc ion batteries. *Microstructures* **2025**, *5*, 2025018. https://dx.doi.org/10.20517/microstructures.2024.47

Received: 30 May 2024 **First Decision:** 2 Aug 2024 **Revised:** 17 Aug 2024 **Accepted:** 20 Sep 2024 **Published:** 21 Feb 2025

Academic Editor: Zaiping Guo **Copy Editor:** Fangling Lan **Production Editor:** Fangling Lan

Abstract

With the over-consumption of non-renewable energy, green and clean renewable energy is inevitably the choice in modern society. In particular, lithium-ion batteries (LIBs) have been widely used in automobiles, aviation and other fields due to their high energy density and other advantages. However, lithium reserves are limited, and LIBs have safety hazards, so the development of alternative rechargeable batteries cannot be delayed. Aqueous zinc ion batteries (AZIBs) have a high theoretical specific capacity while ensuring safety, and have been intensively investigated in recent years. The advancement of cathode materials is essential for AZIBs. In this article, the recent development of non-oxide manganese and vanadium cathode materials such as MnS, MnHCF, VN, VSe_2 and VS_2 for AZIBs is critically reviewed. The emerging strategies for modifying these cathode materials for enhanced electrochemical performance are critically analyzed. Finally, some important achievements of this research field are summarized, and the challenges and future research directions are presented. We hope that this article can shed light on the development of AZIBs.

Keywords: Renewable energy, aqueous zinc ion batteries, cathode materials, oxygen-free compounds

INTRODUCTION

With the progress of global industrialization, the worldwide demand for energy is increasing, which is accompanied by the excessive consumption of fossil fuels and a series of problems such as environmental pollution[1-3]. Therefore, the development of green, efficient and large-area energy storage systems to fully utilize renewable energy sources has become an inevitable trend for the sustainable development of the global economy and society[4,5]. Among them, large-scale electrochemical energy storage systems have attracted much attention due to their green features, high efficiency, and long lifetime[6]. Currently, there are four main categories in the secondary battery market: lead-acid batteries, alkaline nickel/cadmium batteries, nickel/metal hydride batteries, and lithium-ion batteries (LIBs). Among them, lead-acid batteries and nickel/cadmium batteries are cheap and durable but have low energy density and are associated with environmental pollution and harmful effects[7]. LIBs have been widely used in portable electronic devices, automobiles, aerospace, and other fields since the 1990s because of their high energy density, light weight, durability, and other advantages[8,9]. However, the success of LIBs is not sustainable. Firstly, the low reserves of lithium and the difficulty in extracting it have resulted in an increase in cost; secondly, the organic electrolyte used in LIBs poses serious safety hazards in practice, with numerous reports of fires in new energy vehicles emerging in recent years[10-16]. Unlike organic electrolytes, aqueous electrolytes are safer, cheaper, and have advantages such as high ionic conductivity and easy preparation, which are expected to be applied in the next generation of green secondary batteries[17-19]. Therefore, in order to cope with the long-term development needs, the development of a new type of non-lithium rechargeable aqueous batteries for large-scale energy storage systems is of great strategic significance.

Aqueous rechargeable batteries have flourished in recent years by virtue of their advantages such as easy assembly, environmental friendliness, and low cost[20]. At present, based on the comprehensive consideration of the storage capacity and cost, a variety of aqueous batteries including Na^+, K^+, Zn^{2+}, Ca^{2+}, Mg^{2+}, and $A1^{3+}$ have been developed[21-26]. Among them, Na^+, K^+ and Li^+ batteries are similar in nature and are developing rapidly, which have a tendency to replace LIBs, but their active chemical properties are destined to be accompanied by safety hazards[27]. Although multivalent ions have a high specific capacity and energy density, some issues should be properly addressed. For example, Ca^{2+} batteries exist with anode deposition and dissolution; Mg^{2+} diffusion is slow and magnesium is easy to passivate; $A1^{3+}$ surface is prone to the formation of alumina film leading to a decline in battery performance[28-35]. In contrast, aqueous zinc ion batteries (AZIBs) are able to operate stably in neutral and weakly acidic electrolytes; in addition[36], (1) the positive and negative materials and electrolytes for AZIBs are inexpensive, easy to obtain, and environmentally friendly; (2) zinc, as the negative electrode of the batteries, has a volumetric energy density of 5,855 mAh cm^{-3} and a theoretical specific capacity of 820 mAh g^{-1}; and (3) low redox potential of Zn/Zn^{2+} [-0.76 V *vs.* standard hydrogen electrode (SHE)][37-43]. Therefore, AZIBs will certainly have a place in the energy storage field in the future.

AZIBs, as shown in Figure 1[44], have been developed for a long time[45-49]. In 1799, the Italian scientist Alessandro Volta invented the first battery - voltaic pile using zinc. Then, in 1868, the French engineer Georges Leclain invented the zinc-manganese battery. In 1886, dry cell zinc-carbon batteries appeared. Subsequently, Zn-Ag and Zn-Ni batteries have also been studied one after another. However, the early AZIBs used alkaline solutions as the electrolyte, and the positive and negative electrodes of the batteries were prone to irreversible reactions, resulting in the decline of battery life[50]. It was not until 1986 that Japanese scientists Yamamoto *et al.* first used a weakly acidic zinc sulfate ($ZnSO_4$) electrolyte instead of an alkaline electrolyte to prepare and validate the cycling stability of $Zn|ZnSO_4|MnO_2$ batteries, which opened the door to the development of rechargeable AZIBs[51]. Since then, research on rechargeable AZIBs has focused on neutral or weakly acidic electrolytes, from which a variety of cathode materials have been developed, and the development process is shown in Figure 2A [52-55].

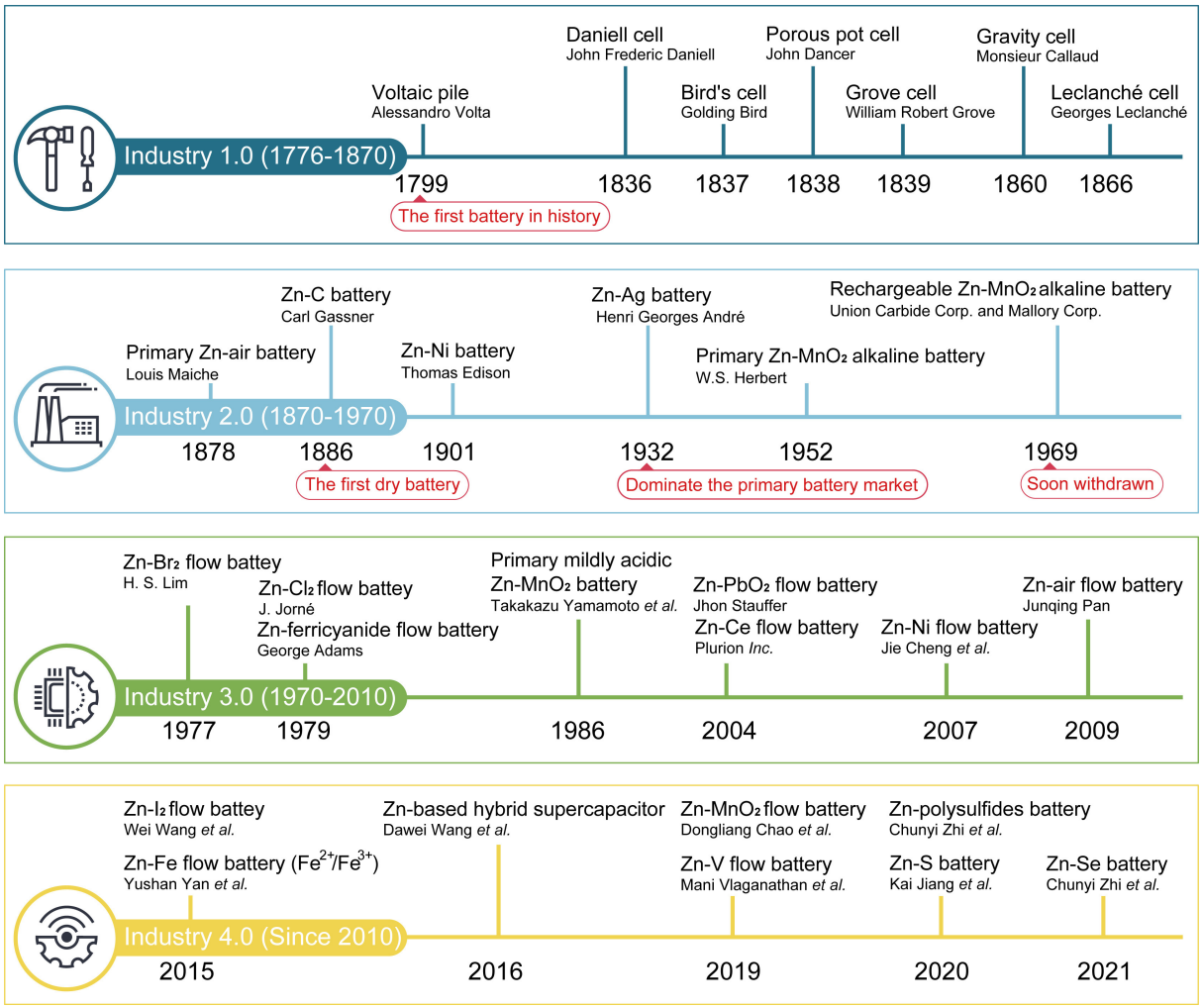

Figure 1. The development history of representative Zn-based EES devices[44]. Copyright 2021, Elsevier.

As the host material of Zn^{2+}, the nature and structure of the cathode material largely determine the performance of the battery. To improve the specific capacity of AZIBs, the development of cathode materials with excellent performance is inevitable[56]. Therefore, the cathode material requires: (1) a suitable structure, including the embedding and detachment of ions, while ensuring the stability of the structure in the process of embedding and detachment; and (2) a suitable zinc storage potential, which is conducive to the occurrence of redox reactions at the positive and negative electrodes. To enhance the electrochemical performance of AZIBs, as shown in Figure 2B, the currently considered ideal cathode materials for AZIBs include manganese compounds, vanadium compounds, and Prussian blue analogs[57-62]. Figure 2C visualizes the advantages and disadvantages of several materials based on different parameters. Compared to manganese-based compounds, as well as Prussian blue and its analogs, vanadium-based compounds offer the benefits of a higher specific capacity and a more stable cycle life. Moreover, they possess a range of crystal structures, such as layered, tunnel, and NASICON types, which promote multi-electron transfer, aid in achieving local electrical neutrality, and mitigate polarization issues arising from Zn^{2+} insertion[54]. However, the development of vanadium oxides has been greatly hindered by the low working voltage of

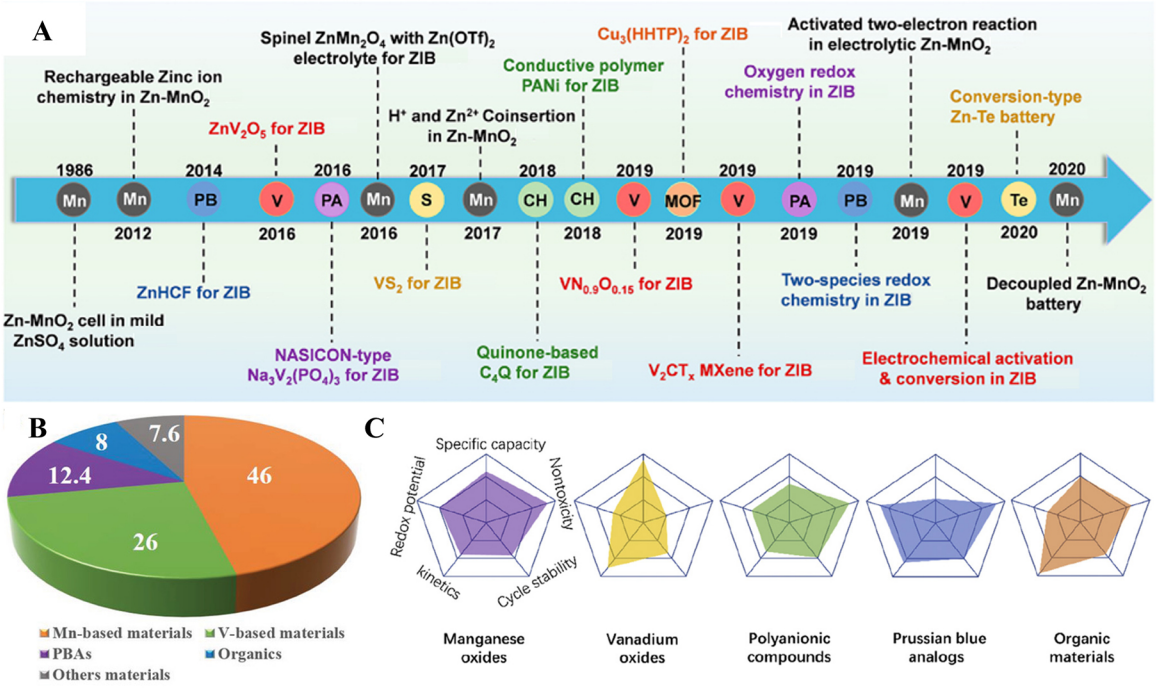

Figure 2. (A) Main progress and brief development history of cathode materials[53]. Copyright 2021, American Chemical Society. (B) Percentage of current ZIB studies on various cathode materials[54]. Copyright 2019, John Wiley and Sons. (C) Characteristics of various ZIB cathode materials[55]. Copyright 2021, Elsevier.

vanadium-based compounds (about 0.8 V compared to Zn^{2+}/Zn), slow reaction kinetics and few reactive active sites[63]. Manganese oxides are abundant, safe and non-toxic, and inexpensive, and exhibit good electrochemical properties. Among them, MnO_2 is favored by researchers for its rich crystalline form. However, the unclear storage mechanisms of manganese-based compounds, coupled with severe electrode dissolution during the charging and discharging process and the ensuing structural damage, reduce the battery life[64-68]. To address these problems, researchers have improved cathode materials through modifications such as capping, ionic pre-embedding, anion/cation vacancies, and morphology modification, which, in turn, improve the battery performance. For example, MnO-carbon nanotube (CNT)@C_3N_4 nanocomposites were developed recently, and the capacity retention rate of the assembled Zn//MnO-CNT@C_3N_4 batteries was 87.5% after 1,000 cycles at 3A g^{-1}[69].

Despite a large number of research methods and measures developed to modify and study oxide cathode materials, prolonged charging and discharging inevitably lead to electrode degradation, undermining the effectiveness of these modifications and greatly hindering the commercialization of AZIBs. Therefore, the development of cathode materials with suitable structures to obtain commercially viable AZIBs is of particular importance. So far, the research on cathode materials for AZIBs has focused more on oxides and less on non-oxide materials. However, some non-oxide materials exhibit superior electrochemical properties compared to oxide materials; e.g., metal sulfides exhibit better electrochemical activity and greater thermodynamic stability; metal selenides have better electrical conductivity and substantial theoretical stacking capacity densities. These properties determine that non-oxide materials will definitely have a place in energy storage, which is well-proven in the remaining metal-ion batteries. For example, Qian *et al.* applied $MnSe_2$ to sodium-ion batteries and prepared $MnSe_2$NCs cathode materials that realized multi-electron pair reactions and showed excellent cycling stability[70]. Therefore, in order to promote the

footsteps of the commercialization process of AZIBs and make up for the application of non-oxide materials in the field of AZIBs, this paper summarizes six existing non-oxide materials to facilitate later researchers to review and summarize [Figure 3].

There is a large amount of literature available on the modification and summarization of manganese oxides and vanadium oxides, so this review article will not go into detail for oxide materials here. After a brief introduction, the recent progress of non-oxide manganese and vanadium compounds is discussed, with a critical analysis on the structure and merits when used as positive electrode materials for AZIBs. In addition, the recent development of emerging strategies for further enhancing the specific capacity and cycling performance of these materials is also reviewed. This review will conclude with a summary of the recent development of this research field. The key challenges and perspectives are also presented. We hope that this article will provide useful information for researchers working in relevant fields.

MN-BASED MATERIALS

Manganese-based compounds are popular for their high theoretical specific capacity (308 mAh g^{-1}) and abundant valence states (+2, +3, +4, +7) in a variety of positive grade materials. Among them, MnO_2 alone has seven crystal types (β-, α-, γ-, R-, t-, δ-, and λ-), and it has been demonstrated that diverse crystal types have varying electrochemical properties. In addition, MnO, Mn_2O_3, Mn_3O_4, and some manganates derived from divalent and trivalent Mn elements are also used as electrode materials[71,72]. Although numerous manganese oxides are widely used as cathode materials, manganese-based cathodes exhibit poor cycling stability during charging and discharging, while the energy storage mechanism for manganese oxides is still not unified. Therefore, there is a need to develop non-oxide manganese-based materials to side-by-side validate their energy storage mechanism and fully exploit the non-oxide materials themselves with excellent electrochemical properties.

MnS

In recent years, transition metal sulfides have been gradually researched and developed as positive electrode materials due to their excellent electrochemical properties and abundant reserves in the earth. These sulfides have better thermal stability, electrical conductivity, and reversibility than metal oxides. The interlayer van der Waals force of metal sulfides is weaker. Moreover, the chemical bonding of M-S is weaker than that of M-O, which greatly facilitates the embedding and detachment of ions during charging and discharging. Among various metal sulfides, MnS is of great interest to researchers because of its low cost, stable mechanical properties, and excellent theoretical specific capacity[73-76].

MnS is the main form of manganese sulfide, which is a p-type semiconductor with three different crystalline forms. The X-ray diffraction (XRD) patterns and spatial models of MnS are shown in Figure 4: including the presence of α-MnS (space group Fm3m, a = b = c = 5.224 Å), β-MnS (space group F-43m, a = b = c = 5.615 Å) and γ-MnS (space group P63mc, a = b = 3.97 Å and c = 6.446 Å)[77]. Among them, α-MnS is a thermodynamically stable cubic rock salt type with a green color; β-MnS and γ-MnS are both substable with a pink color; when the temperature is higher than 100 °C or in a high-pressure condition, both substable β-MnS and γ-MnS will be transformed into stable α-MnS[78]. Although α-MnS has an octahedral stable structure, the substable γ-MnS has the best electrochemical performance among the three crystalline forms[79]. γ-MnS has a layered structure that is more conducive to ionic embedding and electrolyte penetration behavior, and has a higher Gibbs free energy that makes the conversion reaction easier during charging and discharging.

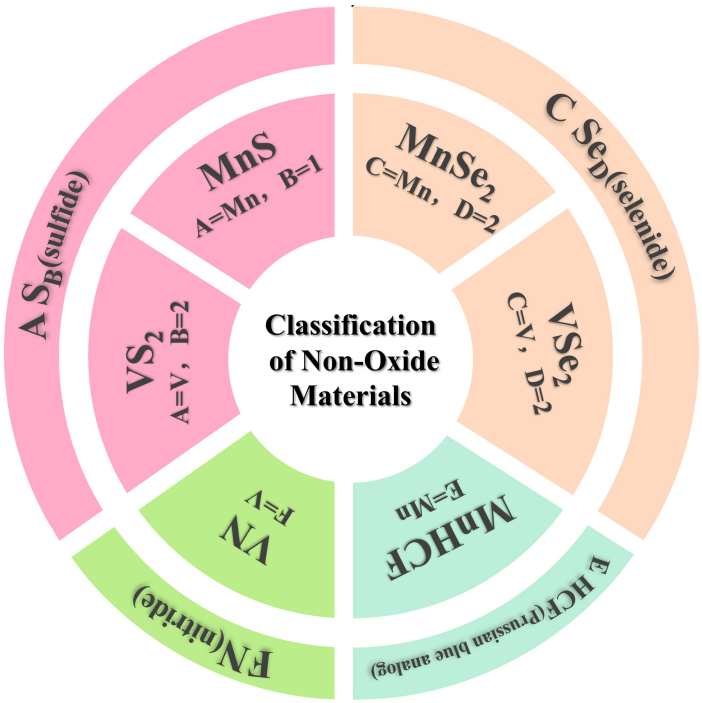

Figure 3. Classification of non-oxide materials.

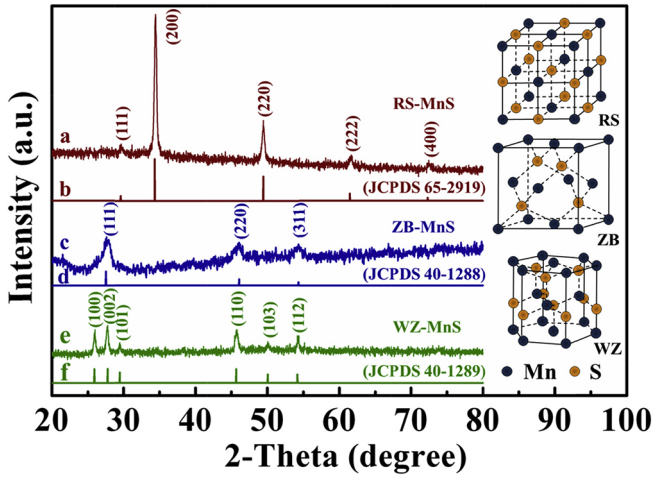

Figure 4. XRD patterns of different crystalline forms of MnS and corresponding crystal structure insets[78]. Copyright 2017, Elsevier.

As an electrode material, MnS has a theoretical specific capacity of 616 mAh g^{-1}, a low redox potential of 1.049 V, and is safe, abundant, and environmentally friendly, and thus has been investigated and applied in capacitors, batteries (e.g., sodium, lithium, and zinc batteries), *etc*. The use of MnS in AZIBs has been verified to have excellent electrochemical performance, and the reaction mechanism shows that MnS is converted to manganese oxide after the first charge/discharge. Compared with the direct application of manganese oxide as the cathode material, MnS, as the cathode material, shows more excellent electrochemical performance. For example, Liu *et al*. used MnS as the cathode material of AZIBs[80], and pointed out that the cyclic voltammetry (CV) curve has no reduction peaks but three oxidation peaks in the first cycle, while two reduction peaks and two oxidation peaks appear respectively in the fifth cycle, which

proves that the conversion reaction of MnS occurs during the charging and discharging process, as shown in Figure 5A. It is also pointed out that the first charging capacity at 0.1 A g^{-1} is 663.5 mAh g^{-1}, and the capacity retention rate after 100 cycles at 0.5 A g^{-1} is 63.6%. The possible mechanism of high stability of MnS in the long term is verified by the non-*in situ* XRD characterization [Figure 5B].

Nevertheless, MnS, as an electrode material, undergoes severe volume changes during charging and discharging, leading to the destruction of the structure and the rapid decay of the capacity. Moreover, the low conductivity of sulfide makes the energy storage device less reversible and the theoretical specific capacity cannot be fully released. Therefore, there is still a need to study the modification of MnS to obtain the desired electrochemical performance. Chen *et al.* prepared MnS [MnS-electrochemically derived oxide (EDO)] by a one-step hot-vapor-solid-sulfurization method using α-MnO_2 as a precursor, exhibiting a specific capacity of 335.7 mAh g^{-1} at a 0.3 A g^{-1}, and almost no capacity fading is observed after 100 cycles [Figure 6A][81]. This work points out that the inactive MnS is desulfurized and converted to high-performance MnS-EDO during the charging and discharging process. This conversion leads to a large number of defects in the material, which exposes more active sites and promotes the penetration of the electrolyte. At the same time, the defects reduce the electrostatic interactions between the host and guest, which improves the ionic diffusion kinetics and facilitates the charge transfer, as shown in Figure 6B and C. The synergistic effect between the defects positively affects the electrochemical performance of the battery.

Wang *et al.* prepared a core-shell structure of MoS_2@MnS, which possessed a high specific capacity of discharge (185.6 mAh g^{-1}) and excellent cycling stability (capacity retention of 90.8% after 300 cycles) when applied to AZIBs[82]. Xu *et al.* prepared MnS/C nanosheets via a manganese sulfide-based organometallic precursor, pointing out that MnS transforms into MnO_x after the first charging[83]. It can be seen from Figure 6D that after the initial cycling, the MnS phase disappears rapidly, and elemental S evolves into a high-valent sulfate. At the same time, the MnO_x phase begins to appear, and the subsequent battery behavior is actually a result of the H^+ and Zn^{2+} of MnO_x and Zn^{2+} of MnO_x. Tang *et al.* prepared MnS/MnO@N-CF by electrostatic spinning, which used N-doped carbon fibers as the nitrogen (N) and carbon sources[84]. In addition, dual ionic defects of Mn and S were generated [Figure 6E and F], which made the composite material simultaneously have abundant reactive sites, excellent ion diffusion rate, and exhibited a reversible capacity of 128.7 mAh g^{-1} at a high current density of 2 A g^{-1}. Tang *et al.* used a combination of various modifications to enhance the battery performance dramatically[84]. The synergistic effect between different modification strategies will produce unexpected chemical reactions, which provides new ideas for us to study new electrode materials in depth. Ma *et al.* prepared manganese sulfide/reduced graphene oxide (MnS/RGO) composites by one-step hydrothermal reaction with the help of graphene's good electrical conductivity, which can effectively alleviate the volumetric change after multiple charging and discharging[85]. In addition, this MnS/RGO composite has excellent structure and conductivity, thus exhibiting a discharge specific capacity of 289 mAh g^{-1} at 0.1 A g^{-1}.

In addition, MnS has also been applied to other zinc batteries. For example, Li *et al.* proposed a two-dimensional (2D) ultrathin Co_9S_8/MnS decorated on sulfur/nitrogen co-doped carbon nanosheets (Co_9S_8/MnS-USNC) for the aqueous/all-solid-state zinc-air batteries [Figure 7A][86], which possessed excellent activities for oxygen reduction reaction (ORR) and oxygen evolution reaction (OER), and greatly improved the battery life [Figure 7B]. Wang *et al.* prepared N-doped carbon nanofibers wrapped with metallic manganese and cobalt sulfides (CMS/NCNF). In the application of solid-state zinc-air batteries, excellent battery performance was obtained at different bending angles [Figure 7C-E][87].

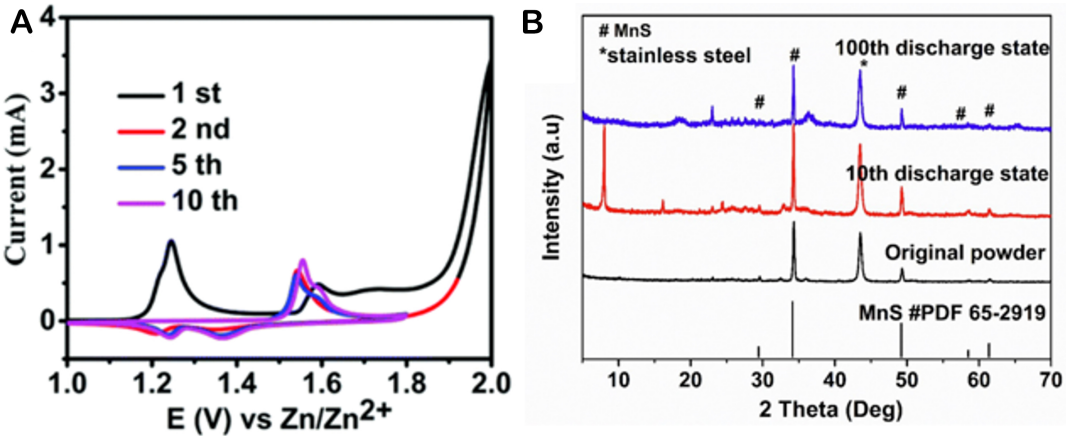

Figure 5. (A) CV images of MnS. (B) *ex situ* XRD of MnS in the zinc ion battery[80]. Copyright 2017, American Chemical Society.

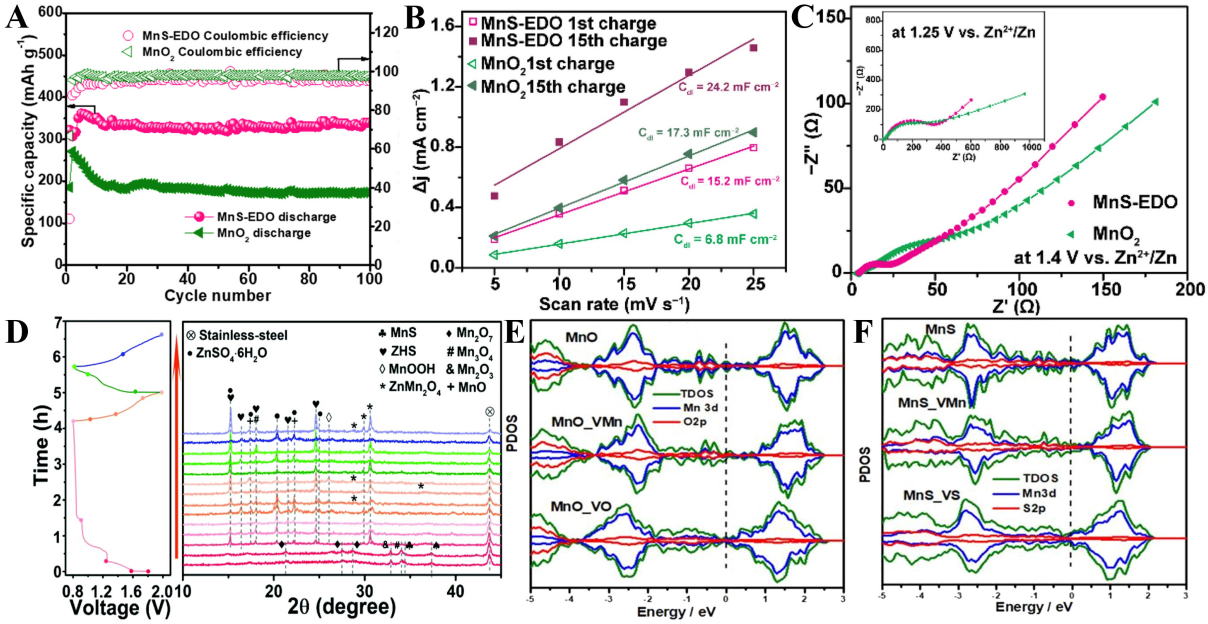

Figure 6. (A) Cyclic stability of MnS-EDO in 1C[81]; (B) Linear fitting results of the difference between anode and cathode current densities *vs.* scanning rate for ECSA estimation of fully charged MnS-EDO and MnO_2 electrodes after cycling for the 1st and 15th turn, respectively[81]; (C) Nyquist plots of MnS-EDO and MnO_2 cathodes at a discharge voltage of 1.40 V (the inset shows Nyquist plots at a discharge voltage of 1.25 V)[81]. Copyright 2020, Elsevier; (D) XRD patterns of MnS/C at different cycling stages in the 1st and 2nd cycles[83]. Copyright 2022, American Chemical Society; (E and F) MnO and Mn defects, MnS and S defects[84]. Copyright 2022, Elsevier.

MnHCF

Prussian blue analogs, also known as metal-ferricyanide compounds (MHCFs), are a class of substances made from Prussian blue through substitution and interstitial modification. The general formula can be expressed as $A_xB_1[B_2(CN)_6]_y$-nH_2O, in which A is an alkali metal ion (e.g., Li, Na, K, Mg, *etc.*) and B is a transition metal (e.g., Mn, Fe, Co, Zn, Ni, *etc.*). The structure of the corresponding Prussian blue analog of Zn^{2+} is shown in Figure 8. Prussian blue was first discovered as a synthetic pigment, and then its analogs were widely used in various types of batteries (e.g., Li, Na, K, Mg, Zn, Al, *etc.*) by virtue of their unique three-dimensional (3D) porous skeleton structure (which facilitates the embedding and dislodging of ions)[88-97].

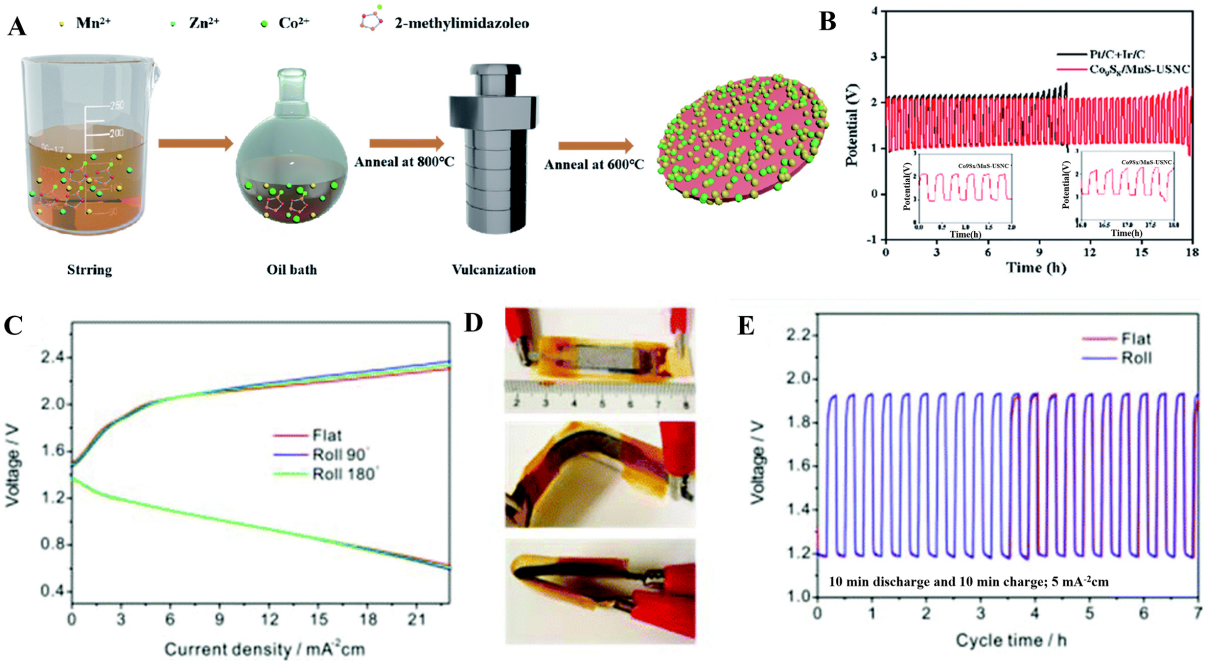

Figure 7. (A) Synthesis route of Co_9S_8/MnS-USNC[86], (B) Cycling stability testing of all-solid-state zinc-air batteries with Co_9S_8/MnS-USNC[86]. Copyright 2021, American Chemical Society. (C-E) Charge-discharge polarization curves, mixed-angle photographs, and electrostatic flow discharge and charge cycling curves at 5 mA cm^{-2} of solid-state zinc-air batteries under CMS/NCNF bifunctional catalysts at different bending angles[87]. Copyright 2017, American Chemical Society.

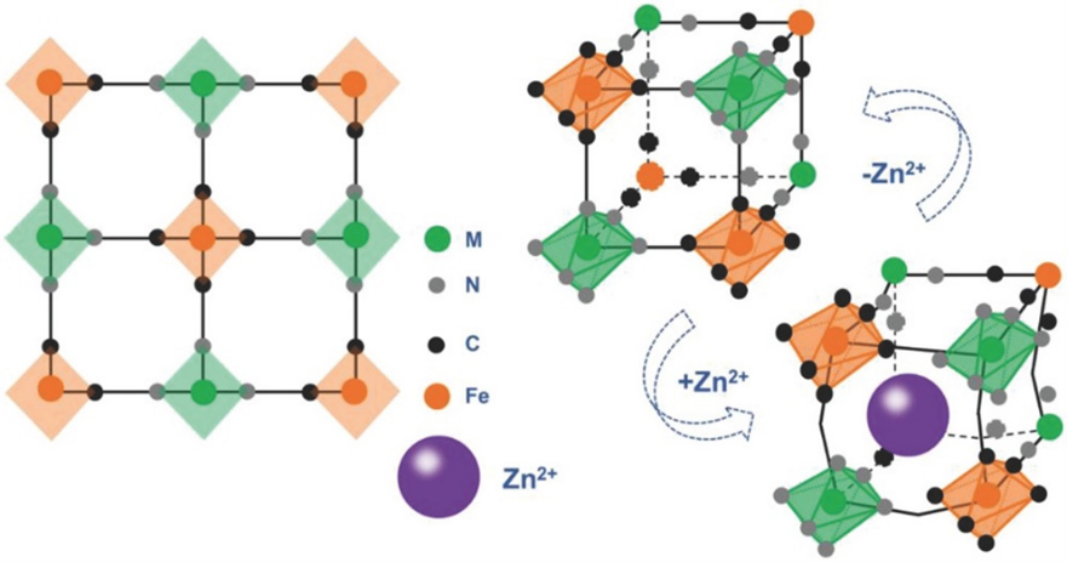

Figure 8. Process of crystal structure change of Prussian blue analogs after Zn^{2+} embedding/de-embedding[97]. Copyright 2018, John Wiley and Sons.

As an electrode material, Prussian blue analogs have the advantages of diverse valence states, sufficient reaction sites, easy synthesis, and unique and stable structure[98]. MnHCF has a higher specific capacity and operating voltage than other Prussian blue analogs, due to the redox reaction of two transition metals (Fe and Mn) in MnHCF and the high spin state of Mn^{HS} exhibiting a high redox potential[99,100]. However,

MnHCF has common disadvantages of manganese-based materials: lattice distortion, manganese dissolution, and poor conductivity of MnHCF, which reacts with electrolytes and seriously hinders the development of MnHCF[101-104]. Li *et al.* assembled a coin cell battery and performed a series of tests using a Zn thin film as the negative electrode, MnHCF and ZnHCF particles as the positive electrode, and 3M $ZnSO_4$ as the electrolyte[105]. The results show that during the charging and discharging process, the capacity contribution of the Fe site gradually increases from 36% to 86%, and the capacity contribution of the Mn site decreases significantly. From Figure 9A, it can be seen that the charging and discharging platform does not change much in the range of 1.0-1.5 v of the Fe reaction voltage. Correspondingly, the charging and discharging platform decreases significantly in the range of 1.5-1.9 voltages. Meanwhile, the structural framework of Zn-C-N-Fe can be detected in the MnHCF samples, which is well characterized in Figure 9B. This is also evidenced by the fact that the oxidation state curve of Fe in Figure 9C almost coincides with the original sample. It indicates that the dissolution of Mn occurs, resulting in the replacement of the Mn sites by Zn, which leads to a decrease in the capacity of the battery during cycling. As a result, the capacity retention rate is only 32.2% at 100 cycles [Figure 9D].

Therefore, some necessary research tools are needed to solve these problems, such as (1) addition of surfactants: Liu *et al.* prepared ultrafine MnHCF with few vacancies and low water content by adding surfactant PAA-K, which can control the size of MnHCF during synthesis and regulate the crystallization process (the synthesis process is shown in Figure 10A)[106]. The assembled battery was tested to possess a high capacity of 139.2 mAh g^{-1} at 0.05 A g^{-1}, while the capacity retention rate was as high as 84.5% after 1,000 cycles at 0.5 A g^{-1}; (2) Impurity element doping: Xue *et al.* introduced zero-dimensional N-doped carbon dots (NCDs) into MnHCF [Figure 10B][107], which significantly improved the conductivity and alleviated the volume change of MnHCF during charging and discharging. The introduction of NCDs provided abundant active sites, which led to the composites exhibiting excellent structural stability. The capacity of MnHCF/NCDs composites as cathodes was as high as 131.2 mAh g^{-1} at 0.05 A g^{-1} and the capacity retention rate was 91% after 1,000 cycles at 1 A g^{-1}. The capacity retention rate was 91% after 1,000 cycles at 1A g^{-1}; (3) Improved electrolyte: the electrolyte is an integral part of the battery, and its properties will also determine the overall performance of the battery. Chen *et al.* constructed a solvated structure of propylene carbonate (PC)-Otfluoromethane sulfonate (Otf)-H_2O[108]. Figure 10C vividly represents this structure in a cartoon diagram, and the results showed that the incorporation of PC suppressed the phase transition from MnHCF to ZnHCF, and improved the battery's cycling stability. In addition, Tan *et al.* proposed a hydroxylation strategy to increase the battery capacity by activating the inactive redox pairs in MnHCF [Figure 10D][109], and the results showed that the hydroxylated MnHCF could continuously activate the multiple redox centers during charging and discharging, which ensured the capacity and stability of the battery.

Similarly, MnHCF has been used in applications with non-aqueous zinc ion batteries (ZIBs); for example, Li *et al.* assembled a battery using MnHCF as the cathode and zinc as the anode in combination with a zinc-containing non-aqueous electrolyte, which exhibited a long operating time of up to 5,460 h with almost no capacity degradation[110].

$MnSe_2$

As another branch of transition metal compounds, excessive metal selenides (TMSs) have gradually entered the field of energy storage in recent years for their high theoretical specific capacity as electrode materials [The theoretical specific capacity of $MnSe_2$ is 503 mAh g^{-1}, much higher than that of MnO_2 (308 mAh g^{-1})]. In addition to this, TMSs exhibit good electrical conductivity and electrochemical activity and strong thermodynamic stability[111-113]. Various transition metal selenide electrode materials ($MoSe_2$, $FeSe_2$, $CoSe_2$, and $MnSe_2$)[114-117] are applied in sodium-ion batteries, LIBs, and supercapacitors. However, very few ARE applied in AZIBs. Selenium is in the same group as oxygen and sulfur, and metal selenides exhibit similar

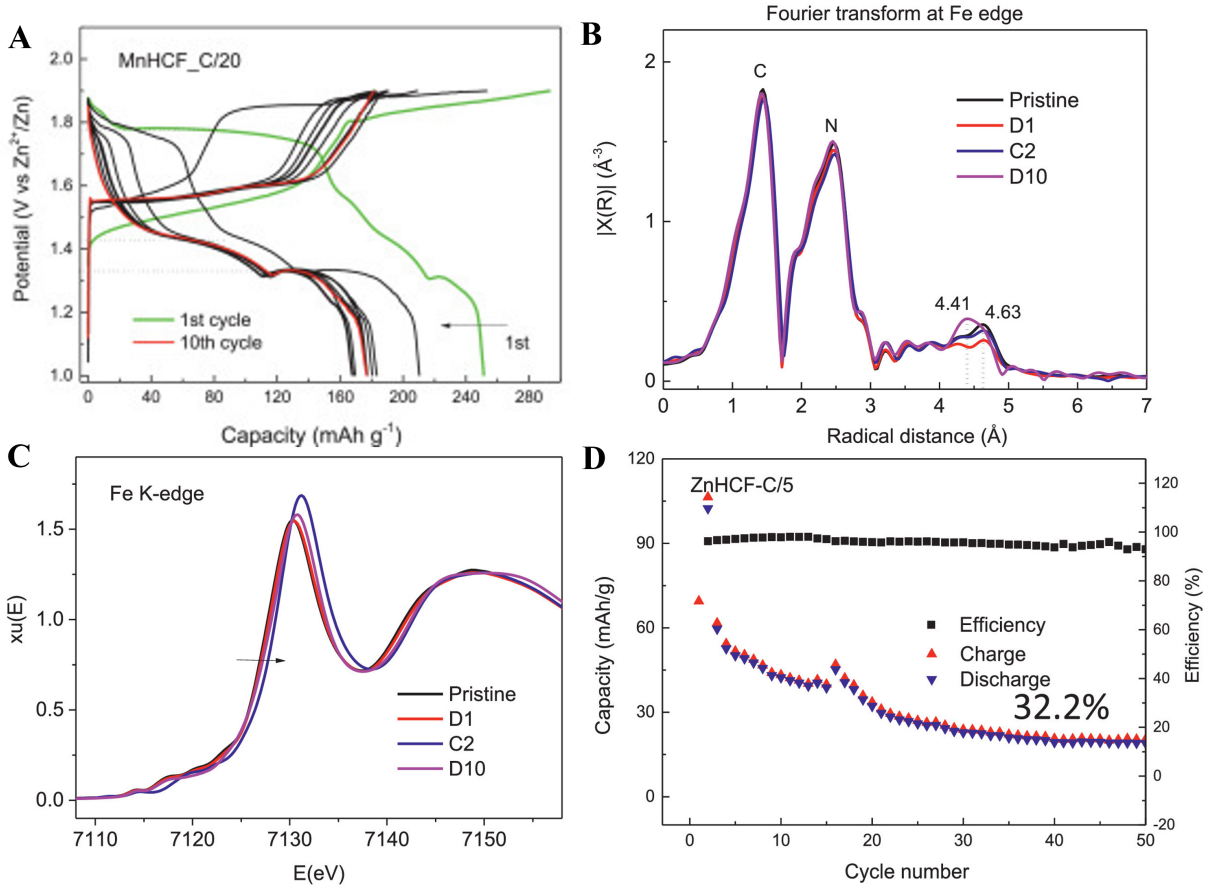

Figure 9. (A) Galvanostatic charge and discharge curves of MnHCF in the initial 10 cycles at C/20; (B) corresponding Fourier transforms (FTs); (C) *ex-situ* XANES of MnHCF powder and the prepared electrodes at the Fe K-edge; (D) cycling performance of ZnHCF at C/5 rate[105]. Copyright 2021, Elsevier.

chemical properties to metal oxides and sulfides, but have better bulk energy density and energy storage advantages. This is because the electrical conductivity and density of metal selenides are better than the remaining two[118-121].

In contrast to $MnSe_2$, MnS, and MnO, Se possesses a larger atomic radius, which gives $MnSe_2$ a larger interlayer spacing and band gap and weaker bonding energy. This structure greatly reduces the difficulty of ion embedding and dislodging during charging and discharging, improves the conversion reaction efficiency, and exhibits better structural stability. Therefore, it is of practical value to develop $MnSe_2$ as a cathode material for AZIBs. However, $MnSe_2$ exhibits severe volume expansion and slow reaction kinetics during charging and discharging, which seriously affects the overall lifetime of the battery for further applications[114]. Therefore, $MnSe_2$ also needs to be modified accordingly to improve its electrochemical stability.

As mentioned above, $MnSe_2$ is not abundantly used in the field of AZIBs, while it has applications in capacitors and sodium-ion and lithium-ion batteries[122]. For example, Ma *et al.* prepared cubic-structured $MnSe_2$ by a disposable hydrothermal method and applied it to supercapacitors, which showed good electrochemical performance; Mukesh *et al.* investigated the effect of Cu-ion doping on the $MnSe_2$ electrode as a material for LIBs, and the results showed that the introduction of Cu ions reduced the bandgap of the

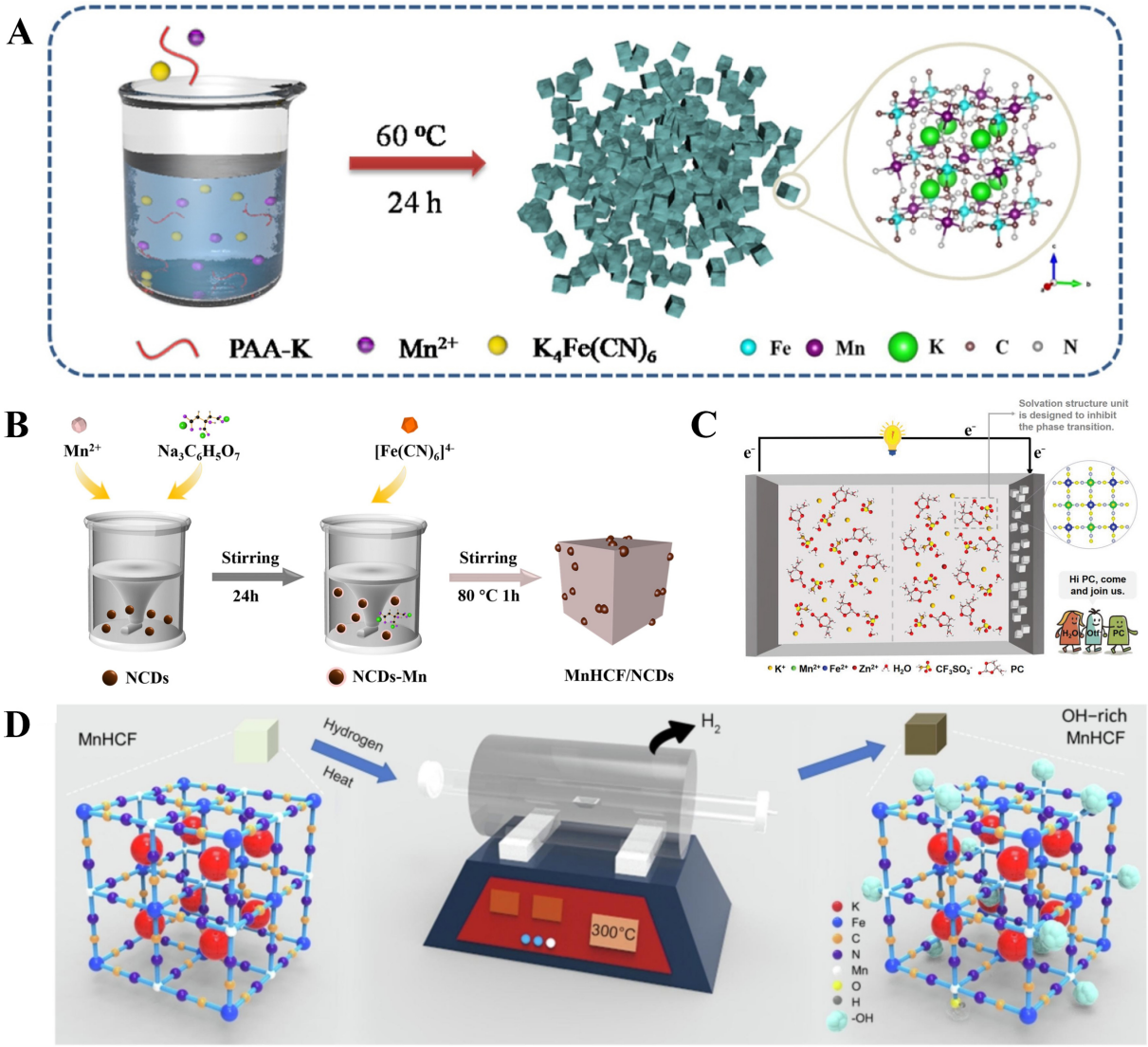

Figure 10. (A) Scheme of the synthetic process of MnHCF/PAA-K[106], Copyright 2023, Elsevier. (B) Scheme for preparing MnHCF/NCDs[107], Copyright 2023, Elsevier. (C) Schematic structure of Zn-MnHCF cell equipped with a novel hybrid electrolyte PC-H_2O co-solvent[108], Copyright 2023, John Wiley and Sons. (D) OH - rich MnHCF synthesis schematic and corresponding structure schematic[109]. Copyright 2023, Elsevier.

material and increased its electrical conductivity; CoS/CoP/NC prepared by Chen *et al.* also showed good electrochemical performance in sodium-ion batteries[123-125].

There are only a few studies on the application of $MnSe_2$ in the field of AZIBs. Xie *et al.* prepared CNTs composite $MnSe_2$/CNTs (MSCN) by a simple one-step room-temperature liquid-phase co-precipitation technique in order to improve the stability of the material and to develop a method suitable for large-scale production [Figure 11A][126]. The article notes that the method enables large-scale production and that the assembled cells maintain high cycling stability at high current densities (87.24% capacity retention after 2,000 cycles at 2A g^{-1}). Li *et al.* prepared $MnSe_2$ with a unique pore structure, and the synthesis method was simple and scaleable, and the Coulombic efficiency remained above 98% after 2,000 cycles [Figure 11B][127]. Premkumar *et al.* prepared $MnSe_2$/PPy electrode materials and applied them to AZIBs by utilizing the

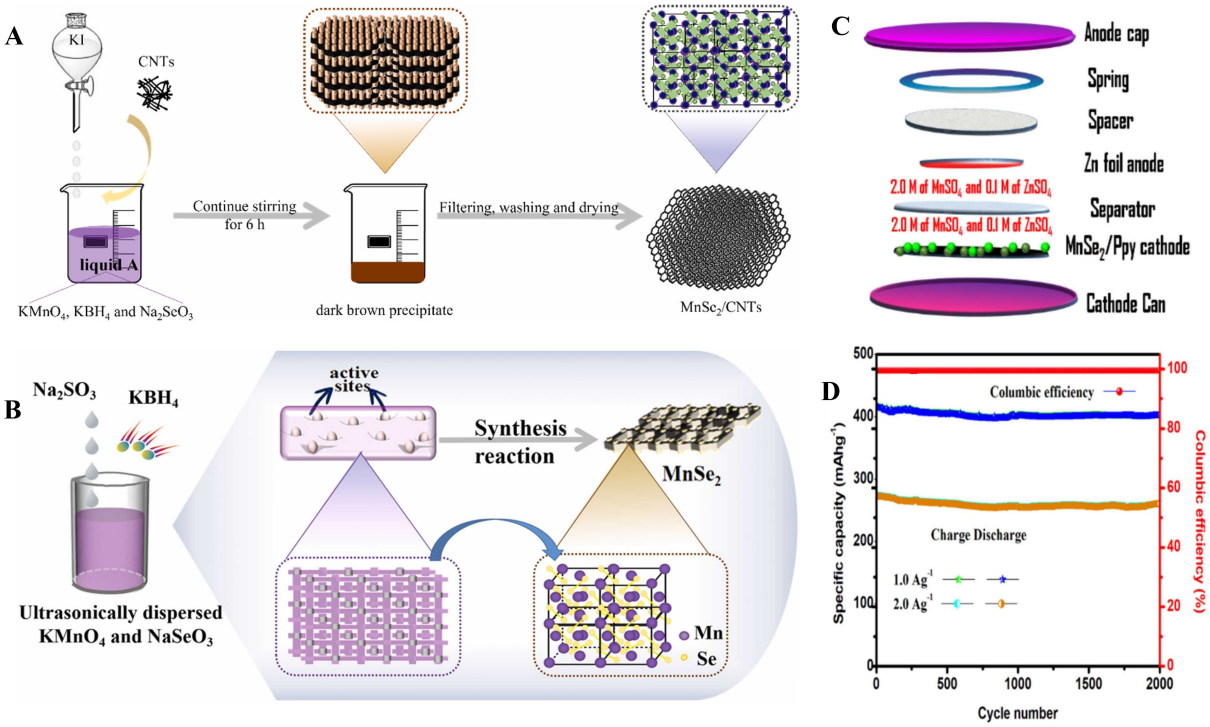

Figure 11. (A) Fabrication process of $MnSe_2$/CNTs (MSCN)[126], Copyright 2023, Elsevier. (B) $MnSe_2$ with special void structure[127], Copyright 2023, Elsevier. (C) $MnSe_2$/PPy cell composition, (D) Long cycle stability of $MnSe_2$/PPy cells[128]. Copyright 2024, Elsevier.

ability of polypyrrole (PPy) to broaden the distribution of active sites in the materials and improve the stability of the composites[128]. The material has sufficient ductility to accommodate volume changes during charging and discharging, thus ensuring good electrochemical performance. The assembled cell exhibited a high specific capacity of up to 283.4 mAh g^{-1} at a current density of 2 A g^{-1}, a capacity retention of 86.3% after 2,000 cycles, and a Coulombic efficiency of close to 100% (99.4% in practice, Figure 11C and D).

To summarize the existing studies, $MnSe_2$ does exhibit good electrochemical properties as an electrode material; however, the volume expansion during charging and discharging seriously hinders the development of this material. Therefore, further consideration is required on how to modify $MnSe_2$ and how to apply the research methods of existing systems to $MnSe_2$ to obtain electrode materials with good stability.

By comparing the three materials mentioned above, it is easy to see that not all non-oxide materials have better electrochemical properties than oxide materials. This is reasonable. First of all, for oxide materials, there has been a great deal of research and modification, which dictates that the best synthesis and testing methods for their materials have been explored. In addition, a large number of investigated modifications have largely improved the electrochemical properties of manganese oxide materials, compensating, to some extent, for the deficiencies of the oxides. However, it can be found that MnO_x formed during charging and discharging processes will show better basic performance than direct synthesis of manganese oxides; for MnHCF, its structure determines the principle of multi-electron pair charging and discharging; the electrochemical properties of $MnSe_2$ approach and even surpass those of manganese oxide materials. All of the above suggests a huge potential for energy storage for non-oxide materials. Meanwhile, for the various studies mentioned in the paper, it can be found that the modification methods are interoperable between

different materials; however, due to the difference in microscopic particles, which determines the difference in properties, further research is still needed on how to apply the modification strategies of oxide materials to non-oxides. Table 1 summarizes the properties of the above-mentioned materials, while a more recent manganese oxide study is introduced to facilitate a visual comparison[65,80-85,105-108,126-129].

VANADIUM-BASED MATERIALS

Owing to the abundance of vanadium resources and its various oxidation states, a diverse array of vanadium-based compounds have been developed. Vanadium compounds exhibit structures such as tetrahedral, pyramidal, trigonal, and octahedral, which typically change based on the oxidation state of vanadium (e.g., V^{5+}, V^{4+}, V^{3+}). In comparison to manganese-based materials and Prussian blue analogs, most vanadium-based cathodes exhibit higher capacity[130,131].

Vanadium nitrides

In the process of cycling, zinc ions encounter issues such as decreased capacity and slow transport kinetics[132,133]. In recent years, vanadium nitride (VN) cathode materials with a cubic structure have emerged as a potential breakthrough to solve these challenges[134,135]. In the initial charging cycle, VN-based materials undergo a high potential inverse reaction, subsequently demonstrating high capacity performance in the second cycle. VN has a face-centered cubic (fcc) structure and exhibits good electrical conductivity and spatial structure[136]. Rong *et al.* synthesized very stable VN particles by reducing and nitrating V_2O_5 through simple solvothermal, calcination and nitration methods in NH_3 atmosphere[137]. A large number of pores exist between the VN particles formed on the typical V_2O_5 core-shell structure. This loose and porous structure enables the VN electrode material to have excellent electrochemical performance. The specific capacity of VN particles is 496 mAh g^{-1} at 0.1 A g^{-1}. Even at a very high current density of 20 A g^{-1}, a specific capacity of 153 mAh g^{-1} can be achieved and a specific capacity of 82 mAh g^{-1} can be maintained after 8,000 cycles. In addition, the prepared VN particles exhibit excellent rate performance when tested at different current densities. The cycling performance of the obtained VN is even better than that of its commercial counterpart. Atomic doping was able to significantly improve the conductivity of vanadium-based compounds and increase the transport rate of Zn^{2+}.

Park *et al.* generated reduced graphene oxide composite (VN-rGO) microspheres with 3D porous structure by spray pyrolysis method of synthesized VN after heat treatment in NH_3 atmosphere[135]. The electrochemical performance of VN-rGO was systematically studied, as shown in Figure 12. After the VN phase transition during the initial charging process, the VN-rGO microspheres exhibited unrivaled high capacity (809 mAh g^{-1}) and excellent rate capability (467 mAh g^{-1} at 2.0 A g^{-1}) at 0.1 A g^{-1} [Figure 12A-E]. The 3D porous matrix, in turn, refines structural stability, which is mainly reflected in the cathode's ability to maintain a specific capacity of 445 mAh g^{-1} even after 400 cycles at 1.0 A g^{-1}, along with a high energy density (613 Wh kg^{-1}) [Figure 12F and G]. The VN-rGO microspheres have a high electrical conductivity that can accelerate the storage of Zn^{2+} ions to obtain high capacity and enhance the structural stability of the material.

Zhang *et al.* synthesized composites with a 3D self-supporting skeleton and VN as a nitrogen source-doped carbon nanofibers (VN/N-CNFs) by electrostatic spinning and a two-step thermal treatment with pre-oxidation and carbonization[138]. The electrochemical characterization of this material and the analysis of the study lead to the conclusion that the presence of a vanadium-based metal-organic framework (v-MOF) facilitates the *in situ* hierarchical growth of the whisker-like secondary structure, which allows the material to maintain a good structure under thermal stresses. In addition, the 0D-activated VN nanoparticles are homogeneously distributed in both the backbone nanofibers and the branched nanowhiskers. The v-MOF

Table 1. Summary of manganese-based materials in this paper

Products	Potential window (V)	Electrolyte	Initial capacity (mAh g^{-1}; A g^{-1})	Cycles numbers	Capacity retention	Ref.
MnO-CNT@C_3N_4	0.8-1.8	2M $ZnSO_4$ + 0.2M $MnSO_4$	209 (0.8)	200	96%	[65]
MnS	1.0-1.8	$ZnSO_4$	110 (0.5)	100	63.6%	[80]
MnS-EDO	0.8-2.0	2M $ZnSO_4$ + 0.1M $MnSO_4$	335.7 (0.3)	100	100%	[81]
MoS2@MnS	0.0-3.0		185.6 (1.0)	300	90.8%	[82]
MnS/C	0.8-1.8	2M $ZnSO_4$ + 0.1M $MnSO_4$	51.9 (3.0)	1,000	70%	[83]
MnS/MnO@NCF	1.0-1.8		151.0 (0.5)	400	100%	[84]
MnS/RGO	0.8-1.9	2M $ZnSO_4$ + 0.1M $MnSO_4$	62 (3.0)	1,000	70.8%	[85]
MnHCF	1.0-2.0	3M $ZnSO_4$		50	70%	[105]
MnHCF-15	1.0-2.0	3M $Zn(CF_3SO_3)_2$	115.6 (0.1)	1,000	92.5%	[106]
MnHCF/NCDs	0.5-2.0	2M $ZnSO_4$	22.1 (1.0)	1,000	91%	[107]
OH-rich MnHCF	0.9-1.95	2M $Zn(CF_3SO_3)_2$	135.9 (0.05)			[108]
$MnSe_2$/CNTs	0.8-2.0	2M $ZnSO_4$ + 0.1M $MnSO_4$	259.2 (2.0)	2,000	87.24%	[126]
$MnSe_2$	0.8-2.0	2M $ZnSO_4$ + 0.1M $MnSO_4$	231.5 (2.0)	2,000	86.3%	[127]
$MnSe_2$/PPy	0.8-2.0	0.1M $ZnSO_4$ + 2M $MnSO_4$	283.4 (2.0)	2,000	86.3%	[128]
NCMO	0.8-1.9		200 (2.0)	1,000	100%	[129]

obtained *in situ* can both prevent the self-aggregation of highly active 0D nanoparticles, and act as a kind of shell that reduces the dissolution of vanadium during the reaction by controlling the contact with the water-based electrolyte, producing protective and conductive effects. At the same time, this flexible and self-contained electrospun nanofiber woven carbon frame can largely maintain the integrity of the battery structure, and the cell exhibits an ultra-long cycle life with a stable capacity of 482 mAh g^{-1} even after 30,000 cycles at 50 A g^{-1} since pre-activation of the ZIB by cycling it for five revolutions at low current densities. The cathode of the VN/N-CNFs possesses a very good multiplicity performance at 100 A g^{-1} with a high multiplicity discharge capacity of 297 mAh g^{-1}.

Yuan *et al*. modulated the morphology of VN by changing the molar amounts of cetyltrimethylammonium bromide (CTAB), and the anodic phase of the CTAB-modified VN was changed to vanadium oxide (VO_x)[139]. The composite was characterized by the dual energy storage through the "conversion and intercalation reactions" in a wide range of climatic conditions (-15-50 °C), exhibiting excellent rate capacity and cycling stability. During the reaction process, the VN structure can provide a better skeleton for VO_x. Since the N atom has a smaller molar mass compared to the O atom, it can provide a large amount of reaction material for the reaction after the phase transition to increase the capacity. In addition, the porous structure and excellent electrical conductivity of VN can alleviate the volume change and achieve rapid ion transport during the reaction process. The electrochemical performance of this VN-2 cathode was tested and it maintained 393 mAh g^{-1} after 200 cycles at 1 A g^{-1} [Figure 13A]. The VN-2 electrode possesses excellent multiplicative performance at an ultra-high current density of 10 A g^{-1} with a capacity of 427 mAh g^{-1} [Figure 13B]. It also exhibits excellent electrochemical performance of 272 mAh g^{-1} and high cycling stability up to 7,000 cycles at 5 A g^{-1} [Figure 13C], which provides a possibility for further development of AZIBs. Table 2 summarizes the latest vanadium oxide studies with VN performance comparison for review[135,140-145].

VSe_2

Vanadium diselenide (VSe_2) is a typical transition metal disulfide compound metal component with flower-like VSe_2 spheres with an interlayer distance of 6.11 Å. The high electrical conductivity of this material is promising for Zn^{2+} de-embedding[146]; this material has the advantage of high conductivity, but its

Table 2. Comparison of some vanadium-based compounds

Products	Electrolyte	Initial capacity (mAh g^{-1}; A g^{-1})	Cycles numbers	Capacity retention	Ref.
VN-rGO	1M $Zn(CF_3SO_3)_2$	809 (0.1)	400	78%	[135]
V_2O_5	3M $Zn(CF_3SO_3)_2$	319 (0.02)	500	81%	[140]
V_2O_5	1M $Zn(CF_3SO_3)_2$ + 2 M LiTFSI	238 (0.05)	2,000	80%	[141]
δ-$Ni_{0.25}V_2O_5{\cdot}nH_2O$	3M $Zn(CF_3SO_3)_2$	218 (5.0)	1,200	98%	[142]
V_6O_{13}	1M $Zn(CF_3SO_3)_2$	230 (4.0)	3,000	92%	[143]
VO_2(B)	1M $ZnSO_4$	365 (0.05)	200	80%	[144]
VN	3M $Zn(CF_3SO_3)_2$	705 (0.2)	200	60.5%	[145]

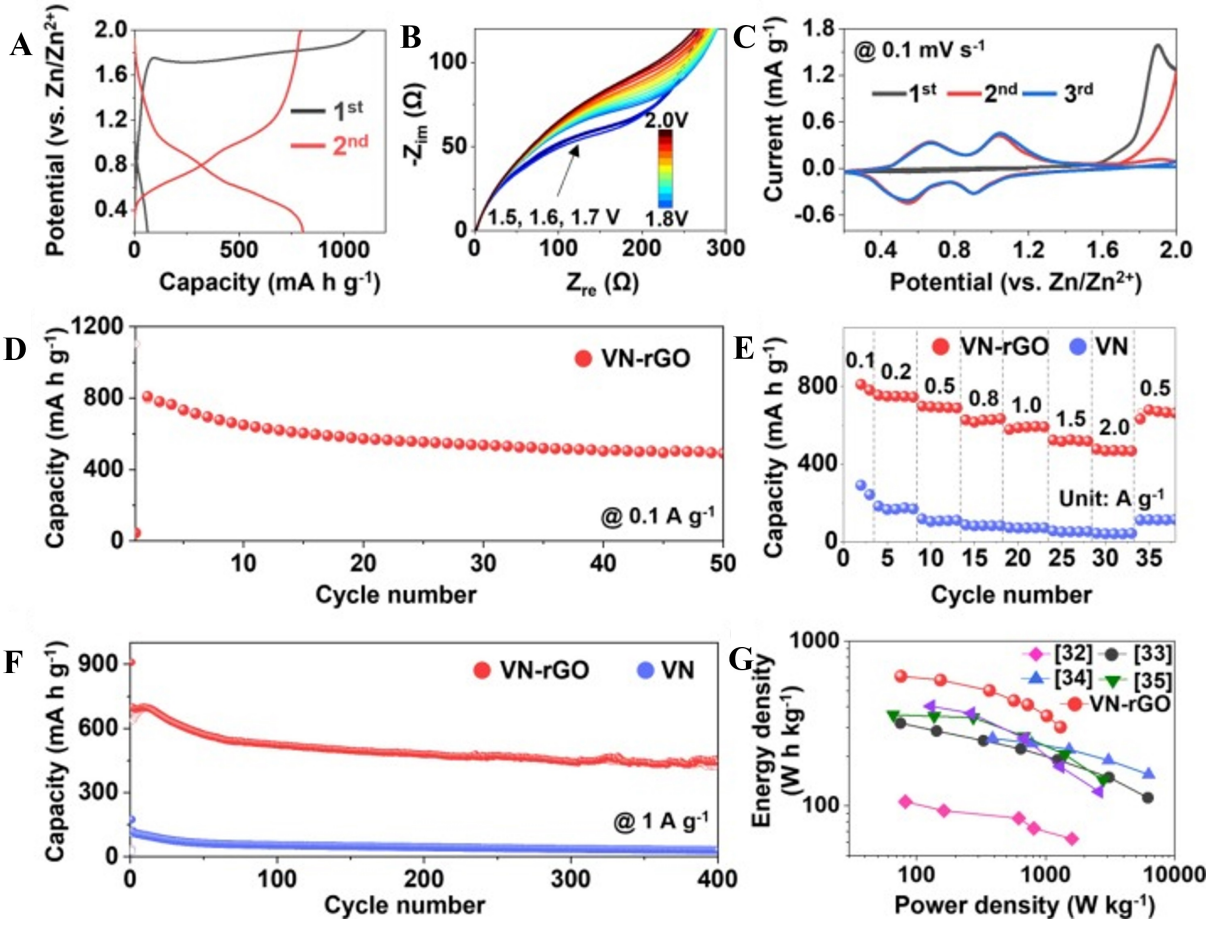

Figure 12. (A) Charge and discharge curves of VN-rGO in the initial two cycles at 0.1 A g^{-1}, (B) *in-situ* EIS plots during the first charging process, (C) CV curve of VN-rGO material for the first three cycles at 0.1 mV s^{-1}, (D) the cycling performance of VN-rGO at 0.1 A g^{-1}, (E) comparison of the rate performance of VN-rGO microspheres and VN microspheres/rods and (F) long cycle performance. (G) comparison of energy density of VN-rGO microspheres with Ragone diagrams of other materials[135]. Copyright 2022, Elsevier.

development still has problems such as low specific capacity (< 200 mAh g^{-1}) and poor rate performance, far lower than vanadium and manganese oxide cathode materials. To solve this problem, defect engineering, thickness reduction and composite formation can improve the Zn^{2+} storage performance of VSe_2. Studies have shown that the creation of selenium defects can well weaken the interfacial adsorption energy barrier, thereby increasing the storage of zinc ions. In addition, the construction of composite materials at the mesoscale can also strengthen the host structure and increase the ion transport rate, thereby improving the

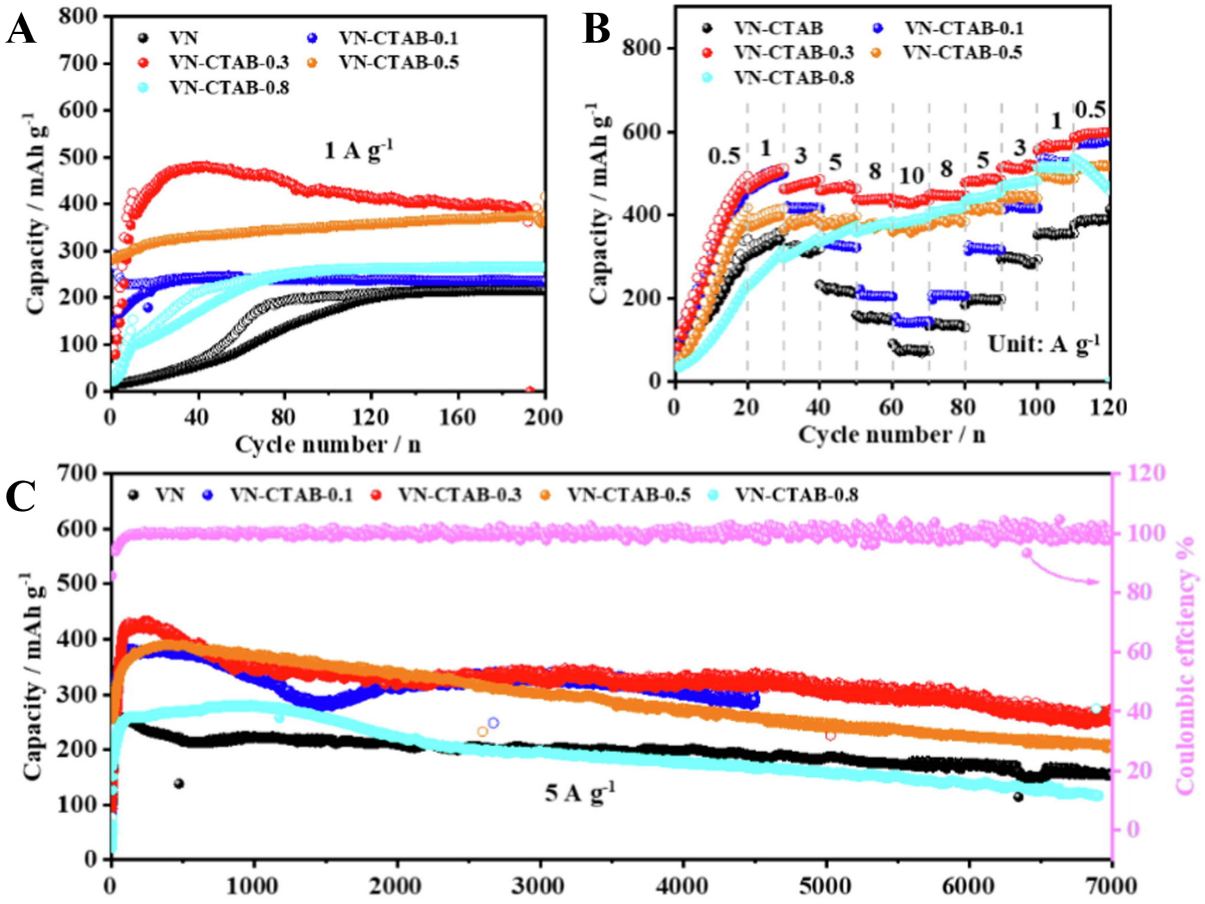

Figure 13. (A and B) Comparison of cyclic properties and magnification properties of different materials at 1 A g^{-1}, (C) long-term cycling properties of various samples at 5 A g^{-1} [139]. Copyright 2023, Elsevier.

cycle stability[147,148]. Moreover, the construction of composites at the mesoscopic scale can also strengthen the host structure and improve the transport kinetics, thus enhancing the cycling stability[149,150].

Bai *et al*. proposed the synthesis of stainless steel (SS) supports with defects (VSe_{2-x}-SS) by hydrothermal reduction to develop VSe_{2-x}-SS nanosheets, an AZIB cathode material with good electrochemical properties, and the creation of Se defects can largely improve the VSe_{2-x}-SS conductivity and activity[147]. Density functional theory (DFT) calculations can demonstrate that the adsorption energy of Zn^{2+} can be modulated by this approach through an effective combination of SS and defect engineering strategies. This suggests that the insertion and extraction of Zn^{2+} ions on VSe_{2-x} is more reversible than pure VSe_2 decorated SS. After 1,800 cycles at 4 A g^{-1}, the specific capacity of VSe_2-x-SS was 175.8 mAh g^{-1}, with a capacity reduction of only 12.2%. However, the capacity of VSe_2-SS was only 75.8 mAh g^{-1}, with a capacity reduction to 65.8% under the same conditions. In addition, the specific capacity of VSe_{2-x}-SS electrodes was 265.2 mAh g^{-1} after 150 cycles at a low current density of 0.2 A g^{-1}, which possesses excellent rate performance and outstanding cycling stability.

Cai *et al*. synthesized VSe_2/Mxene by a facile hydrothermal and calcination process, and the electrochemical performance of VSe_2/Mxene as the cathode material for AZIBs was studied[151]. It was found that oxidation reactions occurred in VSe_2 due to the repeated interaction and extraction of Zn^{2+} and H^+ during the 2,000 cycles. During the reaction, $Zn_{0.25}V_2O_5H_2O$ formed a continuous accumulation on the VSe_2/Mxene surface

[Figure 14A-C], and the accumulation of these nanosheets was responsible for the continuous increase in capacity. The experimental results show that VSe_2/Mxene can provide higher initial specific capacity and faster rate of increase for the cell compared to VSe_2 due to its tiny size.

Yang *et al.* developed a multiscale interfacial structure integrated modulation strategy to tune the interfacial structure of VSe_2 at multiple scales by a one-step hydrothermal stripping method[152]. Theoretical studies show that the combined effect of H_2O embedding and selenium vacancies can largely improve the trapping ability of interfacial zinc ions and reduce the diffusion barrier of zinc ions during the embedding process. The experimental results show that under 0.05 A g^{-1} of 300 cycles, the discharge specific capacity reaches 425 mAh g^{-1} [Figure 15A], and after 5,000 cycles of the VSe_{2-x} nH_2O electrode at 10 A g^{-1}, it still maintains a high performance of 173 mAh g^{-1} [Figure 15B], with an energy density of 258 Whkg^{-1} and a power density of 10.8 kW kg^{-1} [Figure 15C]. Additionally, at 60 °C, it achieves energy and power densities of 465 Wh kg^{-1} and 21.26 kW kg^{-1}, respectively [Figure 15D]. This cathode can be used in a wide range of temperatures (-40 to -60 °C), and exhibits excellent storage performance in both aqueous and solid electrolytes. It also boasts impressive performance in extreme temperature environments, exhibiting a capacity of 122 mAh g^{-1} at -20 °C with a current density of 20 A g^{-1}. The low temperature performance of this experiment is compared with the published articles, as shown in Figure 15E.

VS_2

Vanadium sulfides have a larger layer spacing than oxide and theoretically have a higher diffusion coefficient of zinc ions[153]. These sulfides include VS_2[154-162], VS_4[153,163-165], and V_3S_4[166]. Table 3 gives a summary of potential window, electrolyte and electrochemical performance of vanadium sulfides and their composites.

Transition metal dichalcogenides (TMDs) are a new kind of energy material, structurally similar to graphite.VS_2 is a main representative of TMDs. The large layer spacing (5.76 Å) and high conductivity of VS_2 make it suitable for ZIBs as cathode material; thus, it has also received extensive attention from researchers[167,168].

VS_2 nanosheets were prepared as positive electrode materials by He *et al.*, which had a discharge specific capacity of 190.3 mAh g^{-1} at 0.05 A g^{-1}, and still retained 98% of the initial capacity after 200 cycles at 0.5 A g^{-1}[154]. Meanwhile, the electrochemical reaction of a cathode is divided into two steps[169,170]:

$$VS_2 + 0.09Zn^{2+} + 0.18e^- \rightarrow Zn_{0.09}VS_2 \quad (1)$$

$$Zn_{0.09}VS_2 + 0.14Zn^{2+} + 0.28e^- \rightarrow Zn_{0.23}VS_2 \quad (2)$$

However, it has the disadvantages of poor cycle stability and rate capability. To overcome these shortcomings, the modification of VS_2 has been intensively studied. For instance, a spindle-like VS_2 on a N-doped carbon layer (VS_2@N-C) was synthesized by Zhu *et al.*[161]. The cathode exhibits a superb specific capacity of 203 mA h g^{-1} at a current density of 0.05 A g^{-1} due to strong interfacial interaction between VS_2 and N-doped carbon[161]. Very recently, a one-step hydrothermal method was used to prepare VS_2 with micro-flower shape with appropriate layer spacing. This positive electrode material can provide a stable structure, thus improving the cyclic stability of the reaction[171]. For example, an initial capacity of 128.3 mAh g^{-1} was shown at 3 A g^{-1}, and a discharge capacity of 100.1 mAh g^{-1} remained after 900 cycles. And, the optimized VS_2 microflower also has excellent magnification performance as the cathode of ZIBs.

Table 3. Potential window, electrolyte and electrochemical performance of vanadium sulfide and their composites

Products	Potential window (V)	Electrolyte	Initial capacity (mAh g^{-1}; A g^{-1})	Cycles numbers	Capacity retention	Ref.
VS_2·NH_3	0.2-1.7	2M $Zn(CF_3SO_3)_2$	392 (0.1)	2,000	84.6%	[154]
VS_2@SS	0.4-1.0	1M $ZnSO_4$	149 (0.5)	2,000	80%	[156]
VS_2@VOOH	0.4-1.0	3M $ZnSO_4$	124 (1.5)	350	87%	[157]
rGO-VS_2	0.2-1.8	3M $Zn(CF_3SO_3)_2$	238 (0.1)	1,000	93.3%	[158]
VS_2	0.4-1.4	1M $ZnSO_4$	262 (0.1)	100	81%	[159]
VS_2/VO_x	0.1-1.8	25M $ZnCl_2$	310 (0.05)	3,000	75%	[160]
VS_2@N-C hybrid	0.2-1.8	3M $Zn(CF_3SO_3)_2$	203 (0.05)	600	97%	[161]

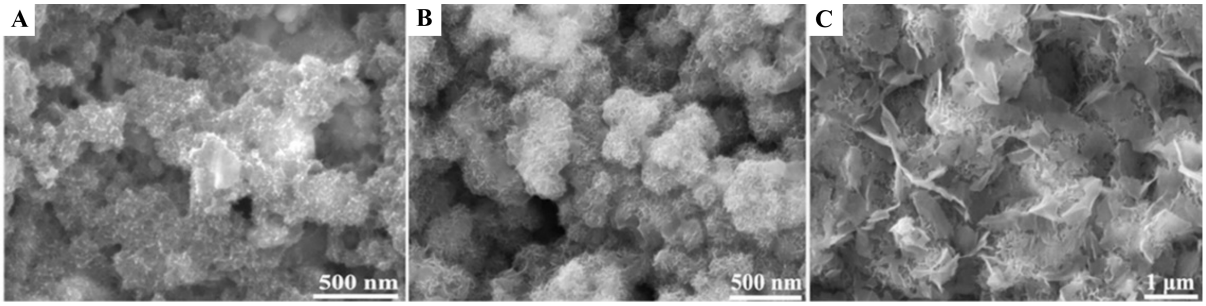

Figure 14. (A-C) The SEM morphology changes of VSe_2/Mxene cathode surface during the reaction process[151]. Copyright 2022, Elsevier.

Samanta *et al*. oxidize VS_2·NH_3 (hollow spheres) to V_2O_5·nH_2O (nanosheets) through an *in-situ* electrochemical oxidation strategy[163]. Because of the existence of vanadium oxide, the resulting cathode has long cyclic stability (110% capacity retention at 3 A g^{-1} after 2,000 cycles)[163].

Another common vanadium sulfide is vanadium tetrasulfide (VS_4), which has chain crystal structure and the active sites are distributed between the layers of chains calculated by DFT[1][166]. Two-step electrochemical reaction of VS_4 is expressed as[172,173]:

$$VS_4 + 0.49Zn^{2+} + 0.98e^- \rightarrow Zn_{0.49}VS_4 \quad (3)$$

$$Zn_{0.49}VS_4 + 0.54Zn^{2+} + 1.08e^- \rightarrow Zn_{1.03}VS_4 \quad (4)$$

Zhu *et al*. prepared VS_4@rGO by combining rGO with VS_4 by one-step hydrothermal method[165].The adding of rGO makes the cathode VS_4@rGO have good cycle stability (82% capacity retention at 10 A g^{-1} after 3,500 cycles) and high specific capacity (450 mA h g^{-1} at 0.5 A g^{-1})[174]. According to the analysis results, the excellent properties of the material are mainly due to the insertion/removal of zinc ions in the VS_4 open channel.

This section enumerates vanadium-based non-oxide modifications that primarily enhance structural stability and improve conductivity during charging and discharging through various heat treatment techniques, including annealing, calcination, heteroatom doping, and surface treatment engineering. Additionally, defect engineering, such as the creation of selenium vacancies, facilitates electron and ion diffusion by adsorbing Zn^{2+} on the material's surface, thereby significantly enhancing the Zn^{2+} storage capacity of vanadium-based compounds for AZIBs. Consequently, further advancements in surface

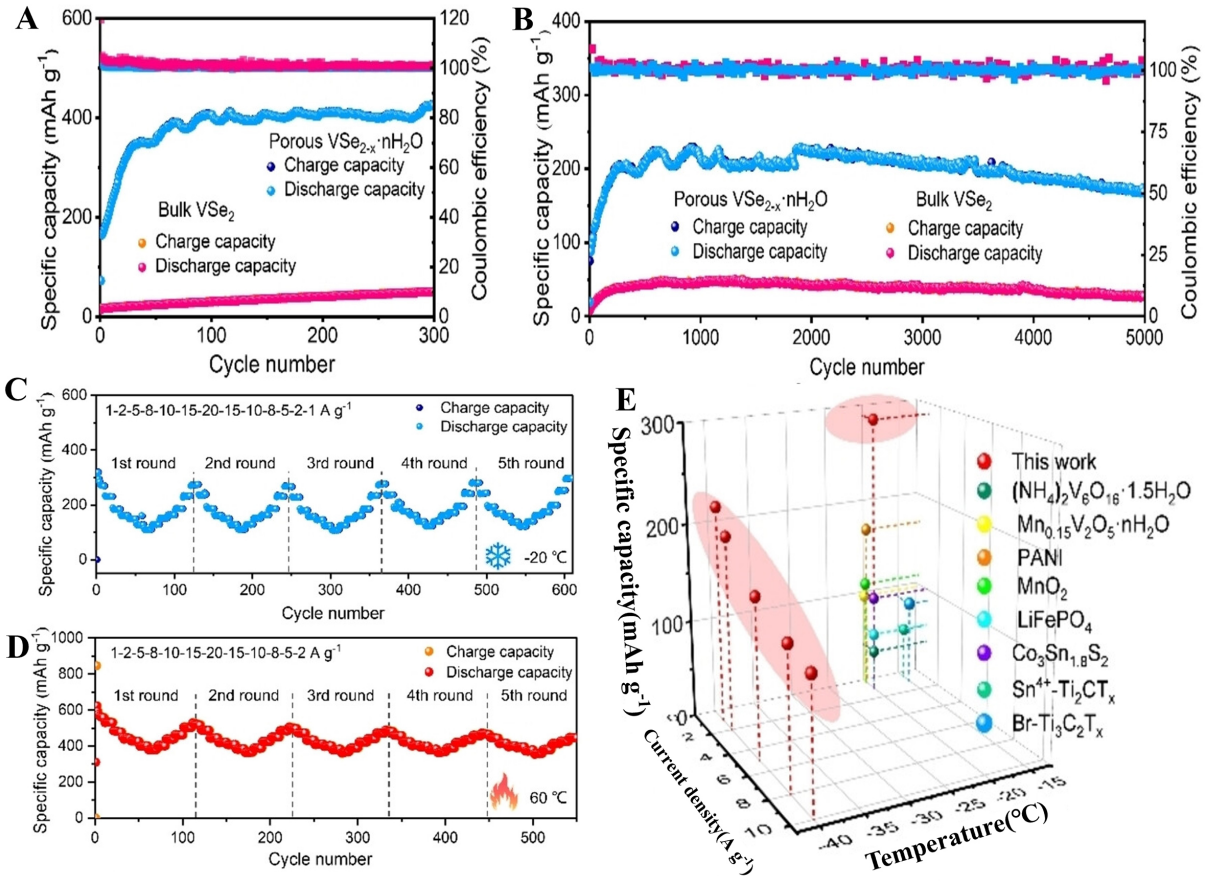

Figure 15. (A and B) Cyclic performance test of the original material VSe_2 and $VSe_{2-x}·nH_2O$ cathode material at 1 A g^{-1} and 10 A g^{-1}, (C and D) rate performance of the battery tested at -20 and 60 °C, (E) comparison of the low temperature performance of this experiment with published articles[152]. Copyright 2023, John Wiley and Sons.

engineering, heteroatom doping, and defect engineering have the potential to significantly enhance the electronic conductivity of vanadium-based compounds and facilitate the migration of ions and electrons within the cathode.

In contrast to the six materials listed above, manganese-based non-oxides are more focused on transition metal compounds. Although transition metals would exhibit better theoretical specific capacities, they have not been well developed so far. With the exception of $MnSe_2$, MnS and MnHCF have so far not shown a tendency to outperform the specific capacity of manganese oxides. However, its reaction mechanism has been preliminarily explored, verifying the possibility of continued development. For example, MnHCF exhibits a multi-electron pair reaction mechanism, and subsequent studies have focused on maintaining the equilibrium between the different electron pairs, rather than accompanying the disappearance of one during charging and discharging. For $MnSe_2$, the structural and electrochemical properties are more favorable and show a tendency to approach manganese oxides, which could perhaps be developed into a commercially available material later with suitable modifications. Compared to the manganese-based compounds described in the article, vanadium-based compounds offer the advantage of rapid adaptation to the insertion/extraction of Zn^{2+}, along with higher specific capacity and superior rate performance. However, as the reaction progresses, the material's interlayer structure is progressively disrupted, resulting in the dissolution of vanadium over an extended period. VN, with its fcc structure, demonstrates excellent

electrical conductivity and a higher discharge specific capacity than VS_2, which, in turn, offers superior long-cycle stability.

SUMMARY AND OUTLOOK

The non-renewable nature of fossil energy dictates that we must develop new sources of energy to cope with the problems that may arise in the future. The distribution of renewable energy sources such as wind and solar is also too irregular, making it difficult to fully utilize them. Therefore, the development of a green and convenient large-scale energy storage system is necessary to cope with possible energy crises. AZIBs adopt aqueous electrolyte, providing a certain degree of environmental safety. Meanwhile, the aqueous electrolyte is cheaper than organic alternatives, and with abundant zinc reserves and high theoretical capacity, AZIBs hold broad application prospects.

However, there are serious interface side reactions and dendrite growth problems in zinc negative electrode, and the electrolyte produces irreversible by-products in the process of charging and discharging, as far as positive electrode materials are concerned:

(1) Dissolution of positive electrode materials: as a common problem of cathode materials, AZIBs will inevitably dissolve cathode materials during charging and discharging, which will lead to loss of the electrode active materials and destroy the structure of the battery, thus leading to the overall performance and cyclicity of the battery.

(2) The electrostatic interaction of divalent zinc ions is larger than that of lithium ions, which makes the embedding and detachment of zinc ions more slow and difficult, and leads to irreversible phase change and structural collapse during repeated charging and discharging, thus affecting the overall performance of the battery.

To date, researchers have proposed a number of modifications to improve the electrochemical performance of aqueous zinc ion cathode materials, including but not limited to shape modulation, ion doping, defect engineering, *etc*. Some progress has also been made in the battery reaction mechanism and other aspects. However, the commercialization of AZIBs still faces various challenges that need to be solved. To speed up this process, this paper puts forward the following immature suggestions:

(1) The unification of the energy storage mechanism of AZIBs: so far, AZIBs operate under four mainstream energy storage mechanisms, Zn^{2+} insertion/extraction, ions/molecules co-insertion/extraction, H^+ insertion/extraction, and conversion reaction mechanisms. These complex reaction mechanisms hinder commercialization. Therefore, there is an urgent need for new characterization techniques to standardize zinc-ion storage mechanisms and analyze their effect on electrochemical performance, enabling more effective modifications to ZIBs.

(2) Explore new cathode materials and improve the existing cathode materials: among existing cathode materials, manganese oxides offer high theoretical specific capacity, but the dissolution of manganese-based materials poses a serious problem, accompanied by lattice distortion and disproportionation reaction, which leads to the destruction of the structure, thus making the performance of manganese-based ZIBs not ideal; vanadium-based compounds, on the other hand, exhibit fewer side reactions and deliver excellent electrochemical performance in the rapid charge and discharge; they can also be used in ZIBs. However, their low discharge voltage [0.4-1.0 V (*vs*. Zn^{2+}/Zn)], and the structural uncertainty of the V-O polyhedra caused by vanadium's many valence states are notable limitations; Prussian blue analogs are simple to

synthesize and have high charge/discharge voltages; however, the poor cycling stability of these batteries and their high cost have greatly hindered commercialization. Therefore, while ongoing efforts to modify existing cathode materials using established techniques are essential, a single modification may not suffice for commercial production. Research into composite modification based on existing studies could broaden the scope of modification strategies.

Simultaneously, it is crucial to accelerate the exploration and development of new materials. The electrostatic interactions of divalent zinc ions are stronger than those of one-valent lithium, sodium ions, which greatly impedes ion embedding in the charging and discharging process of discharging, resulting in lower reaction kinetics and structural collapse of the reaction process. In response to these problems, it is essential to explore structurally stable, electrochemically active cathode materials without delay, such as molybdenum-based oxides, metal phosphides, metal sulfides, *etc*.

(3) A battery consists of a positive electrode, negative electrode, electrolyte and diaphragm, and its performance is closely related to the composition of each component. Therefore, specialized modification research for each part is essential to improve the overall performance of the battery.

(4) At present, battery performance tests are primarily conducted in the laboratory under low-load conditions. However, in the commercial application, the load is inevitably several times higher than that in the laboratory; therefore, ensuring superior performance under high load is a critical aspect of AZIB commercialization that cannot be overlooked.

In addition, some suggestions for the development and research of non-oxide cathode materials are presented here in the hope that they can inspire future researchers and promote the advancement of AZIBs.

(1) Non-oxide materials will show excellent electrochemical properties in some aspects, but some of their inherent defects can seriously damage the structural stability of the material, so it is necessary to study the modification. Whether a large number of existing modification strategies can be directly applied to non-oxide materials needs to be further explored. With respect to the existing research on non-oxide cathode materials, ion doping, surface modification, and defect control are equally practical. However, for different ions, the same modification will produce different effects, so this will require a great deal of future research and development. From the existing findings, it is valuable to conduct such experiments and attempts to enrich the basic research.

(2) For manganese-based non-oxide, its own low price, abundant reserves, safety and non-toxicity are destined to occupy a corner in the future energy storage field. The research on manganese-based non-oxides for AZIBs is still few, while LIBs are already commercially available. For research bottlenecks that cannot be broken through for the time being, it may be incredibly effective to look beyond oxides to non-oxides. A large number of existing studies for manganese oxides can be used as a reference for non-oxide studies. In addition, the study of non-oxides may be able to contribute to the unification of the manganese oxide energy storage mechanism in AZIBs, which, in turn, will promote the development of manganese oxides and realize high-performance commercially available AZIBs.

(3) Several key challenges remain in the research of vanadium-based compounds, including complex energy storage mechanisms and a lower average operating voltage. Inserting metal ions between layers as struts is an effective way to enhance the structural stability of materials. However, the type and amount of pre-inserted metal ions can impede zinc ion insertion and potentially trigger phase transitions. Consequently,

researchers should more thoroughly understand the impact of pre-inserted metal ions on the host material's crystal structure, ensuring the reversibility of Zn^{2+} insertion/extraction through multiple cycles. It is recommended to perform *in-situ* characterization, including *in-situ* transmission electron microscopy (TEM), Raman spectroscopy, and XRD.

(4) The specific capacity of previously reported cathode materials is still lower than the high capacity of zinc anodes (820 mAh g^{-1}). This discrepancy necessitates the discovery of more cathode materials with innovative zinc storage mechanisms to enhance the cycling and rate performance of ZIBs.

(5) Technology has rapidly advanced in recent years, allowing for the exploration of new methods for material synthesis, which may result in materials with different properties. For example, Gao *et al.* summarize several existing compounds synthesized using 3D printing technology in a table. Some manganese-based and vanadium-based compounds synthesized through these techniques also exhibit good electrochemical performance when applied to ZIBs[175]. As the technology matures, it can also be applied to the synthesis of non-oxide materials in future developments.

(6) Although this paper focuses on manganese- and vanadium-based non-oxides, the study of the remaining non-oxide metals should also be expanded. For example, Niu *et al.* prepared a novel MoS_2-double-layer nanotubes (DLTs) material that exhibits abundant defects and a large layer spacing, which provides a good structural advantage for the embedded detachment of ions and ultimately exhibits excellent electrochemical properties[176]. Lu *et al.* successfully prepared MnSe@NC@ReS_2 anode material, which was finally applied to sodium-potassium batteries[177]. This work also provided a new synthesis idea for future materials. This suggests that subsequent research should not limited to existing cathode materials; exploring structures that may exhibit excellent electrochemical properties could prove beneficial.

DECLARATIONS

Acknowledgements

The authors would like to acknowledge material characterizations from the Analytical & Testing Center of Northwestern Polytechnical University.

Authors' contributions

Literature review and writing-original draft: Gao, W.
Figure layout: Feng, J.; Wang, S. (Shuaipeng Wang)
Picture production: Wang, T.
Writing-review & editing, supervision, and funding acquisition: Wang, S. (Songcan Wang)

Availability of data and materials

Not applicable.

Financial support and sponsorship

This work was financially supported by the Ningbo Natural Science Foundation (No. 202003N4054) and the Fundamental Research Funds for the Central Universities.

Conflicts of interest

All authors declared that there are no conflicts of interest.

Ethical approval and consent to participate

Not applicable.

Consent for publication

Not applicable.

REFERENCES

1. Peng, Y.; Bai, Y.; Liu, C.; Cao, S.; Kong, Q.; Pang, H. Applications of metal-organic framework-derived N, P, S doped materials in electrochemical energy conversion and storage. *Coord. Chem. Rev.* **2022**, *466*, 214602. DOI
2. Xiao, X.; Zou, L.; Pang, H.; Xu, Q. Synthesis of micro/nanoscaled metal-organic frameworks and their direct electrochemical applications. *Chem. Soc. Rev.* **2020**, *49*, 301-31. DOI
3. Wang, H. F.; Chen, L.; Pang, H.; Kaskel, S.; Xu, Q. MOF-derived electrocatalysts for oxygen reduction, oxygen evolution and hydrogen evolution reactions. *Chem. Soc. Rev.* **2020**, *49*, 1414-48. DOI PubMed
4. Droguet, L.; Grimaud, A.; Fontaine, O.; Tarascon, J. M. Water-in-salt electrolyte (WiSE) for aqueous batteries: a long way to practicality. *Adv. Energy. Mater.* **2020**, *10*, 2002440. DOI
5. Yi, Z.; Chen, G.; Hou, F.; Wang, L.; Liang, J. Strategies for the stabilization of Zn metal anodes for Zn-ion batteries. *Adv. Energy. Mater.* **2021**, *11*, 2003065. DOI
6. Dunn, B.; Kamath, H.; Tarascon, J. M. Electrical energy storage for the grid: a battery of choices. *Science* **2011**, *334*, 928-35. DOI PubMed
7. Demir-Cakan, R.; Palacin, M. R.; Croguennec, L. Rechargeable aqueous electrolyte batteries: from univalent to multivalent cation chemistry. *J. Mater. Chem. A.* **2019**, *7*, 20519-39. DOI
8. Li, M.; Liu, T.; Bi, X.; et al. Cationic and anionic redox in lithium-ion based batteries. *Chem. Soc. Rev.* **2020**, *49*, 1688-705. DOI
9. Ji, X. A paradigm of storage batteries. *Energy. Environ. Sci.* **2019**, *12*, 3203-24. DOI
10. Xie, J.; Lu, Y. C. A retrospective on lithium-ion batteries. *Nat. Commun.* **2020**, *11*, 2499. DOI PubMed PMC
11. Larcher, D.; Tarascon, J. M. Towards greener and more sustainable batteries for electrical energy storage. *Nat. Chem.* **2015**, *7*, 19-29. DOI PubMed
12. Wang, Q.; Mao, B.; Stoliarov, S. I.; Sun, J. A review of lithium ion battery failure mechanisms and fire prevention strategies. *Prog. Energy. Combust. Sci.* **2019**, *73*, 95-131. DOI
13. Wang, Q.; Jiang, L.; Yu, Y.; Sun, J. Progress of enhancing the safety of lithium ion battery from the electrolyte aspect. *Nano. Energy.* **2019**, *55*, 93-114. DOI
14. Armand, M.; Tarascon, J. M. Building better batteries. *Nature* **2008**, *451*, 652-7. DOI PubMed
15. Liu, X.; Ren, D.; Hsu, H.; et al. Thermal runaway of lithium-ion batteries without internal short circuit. *Joule* **2018**, *2*, 2047-64. DOI
16. Gao, S.; Sun, F.; Liu, N.; Yang, H.; Cao, P. F. Ionic conductive polymers as artificial solid electrolyte interphase films in Li metal batteries - A review. *Mater. Today.* **2020**, *40*, 140-59. DOI
17. Chao, D.; Zhou, W.; Xie, F.; et al. Roadmap for advanced aqueous batteries: from design of materials to applications. *Sci. Adv.* **2020**, *6*, eaba4098. DOI PubMed PMC
18. Peng, Y.; Xu, J.; Xu, J.; et al. Metal-organic framework (MOF) composites as promising materials for energy storage applications. *Adv. Colloid. Interface. Sci.* **2022**, *307*, 102732. DOI
19. Selvakumaran, D.; Pan, A.; Liang, S.; Cao, G. A review on recent developments and challenges of cathode materials for rechargeable aqueous Zn-ion batteries. *J. Mater. Chem. A.* **2019**, *7*, 18209-36. DOI
20. Zhang, H.; Liu, X.; Li, H.; Hasa, I.; Passerini, S. Challenges and strategies for high-energy aqueous electrolyte rechargeable batteries. *Angew. Chem. Int. Ed.* **2021**, *60*, 598-616. DOI PubMed PMC
21. Chen, D.; Lu, M.; Cai, D.; Yang, H.; Han, W. Recent advances in energy storage mechanism of aqueous zinc-ion batteries. *J. Energy. Chem.* **2021**, *54*, 712-26. DOI
22. Ji, B.; He, H.; Yao, W.; Tang, Y. Recent Advances and perspectives on calcium-ion storage: key materials and devices. *Adv. Mater.* **2021**, *33*, e2005501. DOI PubMed
23. Mao, M.; Tong, Y.; Zhang, Q.; et al. Joint cationic and anionic redox chemistry for advanced Mg batteries. *Nano. Lett.* **2020**, *20*, 6852-8. DOI
24. Das, S. K.; Mahapatra, S.; Lahan, H. Aluminium-ion batteries: developments and challenges. *J. Mater. Chem. A.* **2017**, *5*, 6347-67. DOI
25. Wan, F.; Zhou, X.; Lu, Y.; Niu, Z.; Chen, J. Energy storage chemistry in aqueous zinc metal batteries. *ACS. Energy. Lett.* **2020**, *5*, 3569-90. DOI
26. Sun, R.; Xia, P.; Guo, X.; et al. Ternary $Zn_3V_3O_8$ superstructure and synergistic modification of separator promote high performance and stable zinc ion battery. *Chem. Eng. J.* **2024**, *486*, 150377. DOI

27. Li, L.; Zhang, Q.; He, B.; et al. Advanced multifunctional aqueous rechargeable batteries design: from materials and devices to systems. *Adv. Mater.* **2022**, *34*, e2104327. DOI
28. Ponrouch, A.; Frontera, C.; Bardé, F.; Palacín, M. R. Towards a calcium-based rechargeable battery. *Nat. Mater.* **2016**, *15*, 169-72. DOI PubMed
29. Canepa, P.; Sai, G. G.; Hannah, D. C.; et al. Odyssey of multivalent cathode materials: open questions and future challenges. *Chem. Rev.* **2017**, *117*, 4287-341. DOI
30. Ming, J.; Guo, J.; Xia, C.; Wang, W.; Alshareef, H. N. Zinc-ion batteries: materials, mechanisms, and applications. *Mater. Sci. Eng. R. Rep.* **2019**, *135*, 58-84. DOI
31. Sun, X.; Bonnick, P.; Nazar, L. F. Layered TiS_2 positive electrode for Mg batteries. *ACS. Energy. Lett.* **2016**, *1*, 297-301. DOI
32. Sun, X.; Blanc, L.; Nolis, G. M.; Bonnick, P.; Cabana, J.; Nazar, L. F. $NaV_{1.25}Ti_{0.75}O_4$: a potential post-spinel cathode material for Mg batteries. *Chem. Mater.* **2018**, *30*, 121-8. DOI
33. Elia, G. A.; Marquardt, K.; Hoeppner, K.; et al. An overview and future perspectives of aluminum batteries. *Adv. Mater.* **2016**, *28*, 7564-79. DOI
34. Ambroz, F.; Macdonald, T. J.; Nann, T. Trends in aluminium-based intercalation batteries. *Adv. Energy. Mater.* **2017**, *7*, 1602093. DOI
35. Yang, R.; Yao, W.; Tang, B.; et al. Development and challenges of electrode materials for rechargeable Mg batteries. *Energy. Stor. Mater.* **2021**, *42*, 687-704. DOI
36. Pan, Y.; Liu, Z.; Liu, S.; et al. Quasi-decoupled solid-liquid hybrid electrolyte for highly reversible interfacial reaction in aqueous zinc-manganese battery. *Adv. Energy. Mater.* **2023**, *13*, 2203766. DOI
37. Zhao, Y.; Zhou, R.; Song, Z.; et al. Interfacial designing of MnO_2 half-wrapped by aromatic polymers for high-performance aqueous zinc-ion batteries. *Angew. Chem. Int. Ed.* **2022**, *61*, e202212231. DOI
38. Zhang, N.; Cheng, F.; Liu, J.; et al. Rechargeable aqueous zinc-manganese dioxide batteries with high energy and power densities. *Nat. Commun.* **2017**, *8*, 405. DOI PubMed PMC
39. Xu, C.; Li, B.; Du, H.; Kang, F. Energetic zinc ion chemistry: the rechargeable zinc ion battery. *Angew. Chem. Int. Ed.* **2012**, *51*, 933-5. DOI
40. Kim, Y.; Park, Y.; Kim, M.; Lee, J.; Kim, K. J.; Choi, J. W. Corrosion as the origin of limited lifetime of vanadium oxide-based aqueous zinc ion batteries. *Nat. Commun.* **2022**, *13*, 2371. DOI PubMed PMC
41. Xia, C.; Guo, J.; Lei, Y.; Liang, H.; Zhao, C.; Alshareef, H. N. Rechargeable aqueous zinc-ion battery based on porous framework zinc pyrovanadate intercalation cathode. *Adv. Mater.* **2017**, *30*, 1705580. DOI
42. Sun, R.; Dong, S.; Guo, X.; et al. Construction of 2D sandwich-like $Na_2V_6O_{16}\cdot 3H_2O$@MXene heterostructure for advanced aqueous zinc ion batteries. *J. Colloid. Interface. Sci.* **2024**, *655*, 226-33. DOI
43. Guo, S.; Qin, L.; Wu, J.; et al. Conversion-type anode chemistry with interfacial compatibility toward Ah-level near-neutral high-voltage zinc ion batteries. *Natl. Sci. Rev.* **2024**, *11*, nwae181. DOI PubMed PMC
44. Liu, Y.; Lu, X.; Lai, F.; et al. Rechargeable aqueous Zn-based energy storage devices. *Joule* **2021**, *5*, 2845-903. DOI
45. Fang, G.; Zhou, J.; Pan, A.; Liang, S. Recent advances in aqueous zinc-ion batteries. *ACS. Energy. Lett.* **2018**, *3*, 2480-501. DOI
46. Winter, M.; Brodd, R. J. What are batteries, fuel cells, and supercapacitors? *Chem. Rev.* **2004**, *104*, 4245-69. DOI PubMed
47. Zhou, T.; Zhu, L.; Xie, L.; et al. Cathode materials for aqueous zinc-ion batteries: a mini review. *J. Colloid. Interface. Sci.* **2022**, *605*, 828-50. DOI
48. Liang, G.; Mo, F.; Wang, D.; et al. Commencing mild Ag-Zn batteries with long-term stability and ultra-flat voltage platform. *Energy. Storage. Mater.* **2020**, *25*, 86-92. DOI
49. Zhu, X.; Wu, Y.; Lu, Y.; et al. Aluminum-doping-based method for the improvement of the cycle life of cobalt-nickel hydroxides for nickel-zinc batteries. *J. Colloid. Interface. Sci.* **2021**, *587*, 693-702. DOI
50. Qiu, D.; Li, B.; Zhao, C.; et al. A review on zinc electrodes in alkaline electrolyte: current challenges and optimization strategies. *Energy. Storage. Mater.* **2023**, *61*, 102903. DOI
51. Yamamoto, T.; Shoji, T. Rechargeable $Zn|ZnSO_4|MnO_2$-type cells. *Inorg. Chim. Acta.* **1986**, *117*, L27-8. DOI
52. Hu, Y.; Liu, Z.; Li, L.; et al. Reconstructing interfacial manganese deposition for durable aqueous zinc-manganese batteries. *Natl. Sci. Rev.* **2023**, *10*, nwad220. DOI PubMed PMC
53. Wang, X.; Zhang, Z.; Xi, B.; et al. Advances and perspectives of cathode storage chemistry in aqueous zinc-ion batteries. *ACS. Nano.* **2021**, *15*, 9244-72. DOI
54. Chen, L.; An, Q.; Mai, L. Recent advances and prospects of cathode materials for rechargeable aqueous zinc-ion batteries. *Adv. Mater. Inter.* **2019**, *6*, 1900387. DOI
55. Huang, J.; Qiu, X.; Wang, N.; Wang, Y. Aqueous rechargeable zinc batteries: challenges and opportunities. *Curr. Opin. Electrochem.* **2021**, *30*, 100801. DOI
56. Zhang, Z.; Li, W.; Shen, Y.; et al. Issues and opportunities of manganese-based materials for enhanced Zn-ion storage performances. *J. Energy. Storage.* **2022**, *45*, 103729. DOI
57. Tafur, J. P.; Abad, J.; Román, E.; Fernández, R. A. J. Charge storage mechanism of MnO_2 cathodes in Zn/MnO_2 batteries using ionic liquid-based gel polymer electrolytes. *Electrochem. Commun.* **2015**, *60*, 190-4. DOI
58. Hao, J.; Mou, J.; Zhang, J.; et al. Electrochemically induced spinel-layered phase transition of Mn_3O_4 in high performance neutral aqueous rechargeable zinc battery. *Electrochim. Acta.* **2018**, *259*, 170-8. DOI

59. Wei, C.; Xu, C.; Li, B.; Du, H.; Kang, F. Preparation and characterization of manganese dioxides with nano-sized tunnel structures for zinc ion storage. *J. Phys. Chem. Solids.* **2012**, *73*, 1487-91. DOI
60. Pang, Q.; Sun, C.; Yu, Y.; et al. $H_2V_3O_8$ nanowire/graphene electrodes for aqueous rechargeable zinc ion batteries with high rate capability and large capacity. *Adv. Energy. Mater.* **2018**, *8*, 1800144. DOI
61. Lee, H. W.; Wang, R. Y.; Pasta, M.; Woo, L. S.; Liu, N.; Cui, Y. Manganese hexacyanomanganate open framework as a high-capacity positive electrode material for sodium-ion batteries. *Nat. Commun.* **2014**, *5*, 5280. DOI PubMed
62. Chen, X.; Xie, X.; Ruan, P.; Liang, S.; Wong, W. Y.; Fang, G. Thermodynamics and kinetics of conversion reaction in zinc batteries. *ACS. Energy. Lett.* **2024**, *9*, 2037-56. DOI
63. Dou, X.; Xie, X.; Liang, S.; Fang, G. Low-current-density stability of vanadium-based cathodes for aqueous zinc-ion batteries. *Sci. Bull.* **2024**, *69*, 833-45. DOI
64. Liu, S.; Zhu, H.; Zhang, B.; et al. Tuning the kinetics of zinc-ion insertion/extraction in V_2O_5 by in situ polyaniline intercalation enables improved aqueous zinc-ion storage performance. *Adv. Mater.* **2020**, *32*, e2001113. DOI
65. Xu, X.; Xiong, F.; Meng, J.; et al. Vanadium-based nanomaterials: a promising family for emerging metal-ion batteries. *Adv. Funct. Mater.* **2020**, *30*, 1904398. DOI
66. Zuo, S.; Xu, X.; Ji, S.; Wang, Z.; Liu, Z.; Liu, J. Cathodes for aqueous Zn-ion batteries: materials, mechanisms, and kinetics. *Chemistry* **2021**, *27*, 830-60. DOI
67. Gao, Y.; Yin, J.; Xu, X.; Cheng, Y. Pseudocapacitive storage in cathode materials of aqueous zinc ion batteries toward high power and energy density. *J. Mater. Chem. A.* **2022**, *10*, 9773-87. DOI
68. Dong, N.; Zhang, F.; Pan, H. Towards the practical application of Zn metal anodes for mild aqueous rechargeable Zn batteries. *Chem. Sci.* **2022**, *13*, 8243-52. DOI PubMed PMC
69. Xiao, X.; Wang, T.; Zhao, Y.; Gao, W.; Wang, S. A design of MnO-CNT@C_3N_4 cathodes for high-performance aqueous zinc-ion batteries. *J. Colloid. Interface. Sci.* **2023**, *642*, 340-50. DOI
70. Qian, J.; Lau, S. P. $MnSe_2$ nanocubes as an anode material for sodium-ion batteries. *Mater. Today. Energy.* **2018**, *10*, 62-7. DOI
71. Li, G.; Sun, L.; Zhang, S.; et al. Developing cathode materials for aqueous zinc ion batteries: challenges and practical prospects. *Adv. Funct. Mater.* **2024**, *34*, 2301291. DOI
72. Zhou, A.; Chi, R.; Shi, Y.; et al. Manganese-based cathode materials for aqueous rechargeable zinc-ion batteries: recent advance and future prospects. *Mater. Today. Chem.* **2023**, *27*, 101294. DOI
73. Wang, N.; Zhai, Y.; Ma, X.; Qian, Y. Rationally designed hierarchical MnO_2@NiO nanostructures for improved lithium ion storage. *RSC. Adv.* **2015**, *5*, 61148-54. DOI
74. Li, L.; Peng, S.; Bucher, N.; et al. Large-scale synthesis of highly uniform $Fe_{1-x}S$ nanostructures as a high-rate anode for sodium ion batteries. *Nano. Energy.* **2017**, *37*, 81-9. DOI
75. Li, J.; Li, J.; Yan, D.; et al. Design of pomegranate-like clusters with NiS_2 nanoparticles anchored on nitrogen-doped porous carbon for improved sodium ion storage performance. *J. Mater. Chem. A.* **2018**, *6*, 6595-605. DOI
76. Gao, M. R.; Xu, Y. F.; Jiang, J.; Yu, S. H. Nanostructured metal chalcogenides: synthesis, modification, and applications in energy conversion and storage devices. *Chem. Soc. Rev.* **2013**, *42*, 2986-3017. DOI
77. Pei, Y.; Liu, C.; Han, Z.; et al. Revealing the impacts of metastable structure on the electrochemical properties: the case of MnS. *J. Power. Sources.* **2019**, *431*, 75-83. DOI
78. Hao, Y.; Chen, C.; Yang, X.; et al. Studies on intrinsic phase-dependent electrochemical properties of MnS nanocrystals as anodes for lithium-ion batteries. *J. Power. Sources.* **2017**, *338*, 9-16. DOI
79. Sakib, M. N.; Ahmed, S.; Rahat, S. M. S. M.; Shuchi, S. B. A review of recent advances in manganese-based supercapacitors. *J. Energy. Storage.* **2021**, *44*, 103322. DOI
80. Liu, W.; Hao, J.; Xu, C.; et al. Investigation of zinc ion storage of transition metal oxides, sulfides, and borides in zinc ion battery systems. *Chem. Commun.* **2017**, *53*, 6872-4. DOI
81. Chen, X.; Li, W.; Xu, Y.; et al. Charging activation and desulfurization of MnS unlock the active sites and electrochemical reactivity for Zn-ion batteries. *Nano. Energy.* **2020**, *75*, 104869. DOI
82. Wang, L.; Tan, X.; Zhu, Q.; et al. The universality applications of MoS_2@MnS heterojunction hollow microspheres for univalence organic or multivalence aqueous electrolyte energy storage device. *J. Power. Sources.* **2022**, *518*, 230747. DOI
83. Xu, S.; Fan, S.; Ma, W.; Fan, J.; Li, G. Electrochemical reaction behavior of MnS in aqueous zinc ion battery. *Inorg. Chem. Front.* **2022**, *9*, 1481-9. DOI
84. Tang, F.; Wu, X.; Shen, Y.; et al. The intercalation cathode materials of heterostructure MnS/MnO with dual ions defect embedded in N-doped carbon fibers for aqueous zinc ion batteries. *Energy. Storage. Mater.* **2022**, *52*, 180-8. DOI
85. Ma, S. C.; Sun, M.; Sun, B. Y.; et al. In situ preparation of manganese sulfide on reduced graphene oxide sheets as cathode for rechargeable aqueous zinc-ion battery. *J. Solid. State. Chem.* **2021**, *299*, 122166. DOI
86. Li, J.; Li, W.; Mi, H.; et al. Bifunctional oxygen electrocatalysis on ultra-thin Co_9S_8/MnS carbon nanosheets for all-solid-state zinc-air batteries. *J. Mater. Chem. A.* **2021**, *9*, 22635-42. DOI
87. Wang, Y.; Fu, J.; Zhang, Y.; et al. Continuous fabrication of a MnS/Co nanofibrous air electrode for wide integration of rechargeable zinc-air batteries. *Nanoscale* **2017**, *9*, 15865-72. DOI
88. Hu, L.; Chen, Q. Hollow/porous nanostructures derived from nanoscale metal-organic frameworks towards high performance anodes for lithium-ion batteries. *Nanoscale* **2014**, *6*, 1236-57. DOI PubMed

89. Imanishi, N.; Morikawa, T.; Kondo, J.; et al. Lithium intercalation behavior into iron cyanide complex as positive electrode of lithium secondary battery. *J. Power. Sources.* **1999**, *79*, 215-9. DOI
90. Chong, S.; Yang, J.; Sun, L.; Guo, S.; Liu, Y.; Liu, H. K. Potassium nickel iron hexacyanoferrate as ultra-long-life cathode material for potassium-ion batteries with high energy density. *ACS. Nano.* **2020**, *14*, 9807-18. DOI
91. Guo, Z. Y.; Li, C. X.; Gao, M.; et al. Mn-O covalency governs the intrinsic activity of Co-Mn spinel oxides for boosted peroxymonosulfate activation. *Angew. Chem. Int. Ed.* **2021**, *60*, 274-80. DOI
92. Zhang, M.; Dong, T.; Li, D.; Wang, K.; Wei, X.; Liu, S. High-performance aqueous sodium-ion battery based on graphene-doped Na_2 $MnFe(CN)_6$-zinc with a highly stable discharge platform and wide electrochemical stability. *Energy. Fuels.* **2021**, *35*, 10860-8. DOI
93. Kuperman, N.; Cairns, A.; Goncher, G.; Solanki, R. Structural water enhanced intercalation of magnesium ions in copper hexacyanoferrate nonaqueous batteries. *Electrochim. Acta.* **2020**, *362*, 137077. DOI
94. Cao, J.; Zhang, D.; Zhang, X.; et al. Mechanochemical reactions of MnO_2 and graphite nanosheets as a durable zinc ion battery cathode. *Appl. Surf. Sci.* **2020**, *534*, 147630. DOI
95. Zhou, Y.; Chen, F.; Arandiyan, H.; et al. Oxide-based cathode materials for rechargeable zinc ion batteries: progresses and challenges. *J. Energy. Chem.* **2021**, *57*, 516-42. DOI
96. Li, W.; Gao, X.; Chen, Z.; et al. Electrochemically activated MnO cathodes for high performance aqueous zinc-ion battery. *Chem. Eng. J.* **2020**, *402*, 125509. DOI
97. Song, M.; Tan, H.; Chao, D.; Fan, H. J. Recent advances in Zn-ion batteries. *Adv. Funct. Mater.* **2018**, *28*, 1802564. DOI
98. Xu, Y.; Zheng, S.; Tang, H.; Guo, X.; Xue, H.; Pang, H. Prussian blue and its derivatives as electrode materials for electrochemical energy storage. *Energy. Storage. Mater.* **2017**, *9*, 11-30. DOI
99. Wang, B.; Liu, S.; Sun, W.; et al. Intercalation pseudocapacitance boosting ultrafast sodium storage in Prussian blue analogs. *ChemSusChem* **2019**, *12*, 2415-20. DOI
100. Bie, X.; Kubota, K.; Hosaka, T.; Chihara, K.; Komaba, S. Synthesis and electrochemical properties of Na-rich Prussian blue analogues containing Mn, Fe, Co, and Fe for Na-ion batteries. *J. Power. Sources.* **2018**, *378*, 322-30. DOI
101. Jiang, X.; Liu, H.; Song, J.; Yin, C.; Xu, H. Hierarchical mesoporous octahedral $K_2Mn_{1-x}Co_xFe(CN)_6$ as a superior cathode material for sodium-ion batteries. *J. Mater. Chem. A.* **2016**, *4*, 16205-12. DOI
102. Kim, H.; Yoon, G.; Park, I.; et al. Anomalous Jahn-Teller behavior in a manganese-based mixed-phosphate cathode for sodium ion batteries. *Energy. Environ. Sci.* **2015**, *8*, 3325-35. DOI
103. Wang, C.; Xing, L.; Vatamanu, J.; et al. Overlooked electrolyte destabilization by manganese (II) in lithium-ion batteries. *Nat. Commun.* **2019**, *10*, 3423. DOI PubMed PMC
104. Zhang, S.; Gu, H.; Pan, H.; et al. A novel strategy to suppress capacity and voltage fading of Li- and Mn-rich layered oxide cathode material for lithium-ion batteries. *Adv. Energy. Mater.* **2017**, *7*, 1601066. DOI
105. Li, M.; Sciacca, R.; Maisuradze, M.; et al. Electrochemical performance of manganese hexacyanoferrate cathode material in aqueous Zn-ion battery. *Electrochim. Acta.* **2021**, *400*, 139414. DOI
106. Liu, B.; Zhao, R.; Zhang, Q.; et al. Ultrafine manganese hexacyanoferrate with low defects regulated by potassium polyacrylate for high-performance aqueous Zn-ion batteries. *J. Energy. Storage.* **2023**, *72*, 108535. DOI
107. Xue, Y.; Zhou, H.; Ji, Z.; et al. In-situ coupling of N-doped carbon dots with manganese hexacyanoferrate as a cathode material for aqueous zinc-ion batteries. *Appl. Surf. Sci.* **2023**, *633*, 157580. DOI
108. Chen, W.; Wu, J.; Fu, K.; et al. Co-solvent electrolyte design to inhibit phase transition toward high performance K^+/Zn^{2+} hybrid battery. *Small. Methods.* **2024**, *8*, e2300617. DOI
109. Tan, Y.; Yang, H.; Miao, C.; et al. Hydroxylation strategy unlocking multi-redox reaction of manganese hexacyanoferrate for aqueous zinc-ion battery. *Chem. Eng. J.* **2023**, *457*, 141323. DOI
110. Li, Q.; Ma, K.; Yang, G.; Wang, C. High-voltage non-aqueous $Zn/K_{1.6}Mn_{1.2}Fe(CN)_6$ batteries with zero capacity loss in extremely long working duration. *Energy. Storage. Mater.* **2020**, *29*, 246-53. DOI
111. Wang, L.; Wang, Z.; Xie, L.; Zhu, L.; Cao, X. An enabling strategy for ultra-fast lithium storage derived from micro-flower-structured NiX (X=O, S, Se). *Electrochim. Acta.* **2020**, *343*, 136138. DOI
112. Miao, C.; Xiao, X.; Gong, Y.; et al. Facile synthesis of metal-organic framework-derived $CoSe_2$ nanoparticles embedded in the N-doped carbon nanosheet array and application for supercapacitors. *ACS. Appl. Mater. Interfaces.* **2020**, *12*, 9365-75. DOI
113. Zhao, B.; Liu, Q.; Wei, G.; et al. Synthesis of $CoSe_2$ nanoparticles embedded in N-doped carbon with conformal TiO_2 shell for sodium-ion batteries. *Chem. Eng. J.* **2019**, *378*, 122206. DOI
114. Pathak, M.; Tamang, D.; Kandasamy, M.; Chakraborty, B.; Rout, C. S. A comparative experimental and theoretical investigation on energy storage performance of $CoSe_2$, $NiSe_2$ and $MnSe_2$ nanostructures. *Appl. Mater. Today.* **2020**, *19*, 100568. DOI
115. Lu, W.; Xue, M.; Chen, X.; Chen, C. $CoSe_2$ nanoparticles as anode for lithium ion battery. *Int. J. Electrochem. Sci.* **2017**, *12*, 1118-29. DOI
116. Zheng, C.; Chen, C.; Chen, L.; Wei, M. A CMK-5-encapsulated $MoSe_2$ composite for rechargeable lithium-ion batteries with improved electrochemical performance. *J. Mater. Chem. A.* **2017**, *5*, 19632-8. DOI
117. Zhang, K.; Hu, Z.; Liu, X.; Tao, Z.; Chen, J. $FeSe_2$ microspheres as a high-performance anode material for Na-ion batteries. *Adv. Mater.* **2015**, *27*, 3305-9. DOI
118. Zhu, S.; Li, Q.; Wei, Q.; et al. $NiSe_2$ nanooctahedra as an anode material for high-rate and long-life sodium-ion battery. *ACS. Appl.*

Mater. Interfaces. **2017**, *9*, 311-6. DOI

119. Ali, Z.; Tang, T.; Huang, X.; Wang, Y.; Asif, M.; Hou, Y. Cobalt selenide decorated carbon spheres for excellent cycling performance of sodium ion batteries. *Energy. Storage. Mater.* **2018**, *13*, 19-28. DOI
120. Gao, J.; Li, Y.; Shi, L.; Li, J.; Zhang, G. Rational design of hierarchical nanotubes through encapsulating $CoSe_2$ nanoparticles into $MoSe_2$/C composite shells with enhanced lithium and sodium storage performance. *ACS. Appl. Mater. Interfaces.* **2018**, *10*, 20635-42. DOI
121. Yin, H.; Qu, H. Q.; Liu, Z.; Jiang, R. Z.; Li, C.; Zhu, M. Q. Long cycle life and high rate capability of three dimensional $CoSe_2$ grain-attached carbon nanofibers for flexible sodium-ion batteries. *Nano. Energy.* **2019**, *58*, 715-23. DOI
122. Sun, R.; Xu, F.; Wang, C. H.; Lu, S. J.; Zhang, Y. F.; Fan, H. S. Rational design of metal selenides nanomaterials for alkali metal ion (Li^+/Na^+/K^+) batteries: current status and perspectives. *Rare. Met.* **2024**, *43*, 1906-31. DOI
123. Chen, L.; Liu, Z.; Yang, W.; et al. Micro-mesoporous cobalt phosphosulfide (Co_3S_4/CoP/NC) nanowires for ultrahigh rate capacity and ultrastable sodium ion battery. *J. Colloid. Interface. Sci.* **2024**, *666*, 416-23. DOI
124. Mukesh, P.; Sagar, G. L.; Brijesh, K.; et al. Impact of copper doping on the electrochemical response of $MnSe_2$ as anode for lithium-ion battery. *J. Mater. Sci. Mater. Electron.* **2024**, *35*, 12630. DOI
125. Ma, S.; Wang, S. Hydrothermally prepared $MnSe_2$ nanosheets as a novel electrode material for supercapacitor. *Meet. Abstr.* **2019**, *MA2019-02*, 37. DOI
126. Xie, J.; Liu, G.; Jiang, X.; Sui, Z.; Gao, S. One-step co-precipitation of $MnSe_2$/CNTs as a high-performance cathode material for zinc-ion batteries. *Ceram. Int.* **2023**, *49*, 10165-71. DOI
127. Li, X.; Xie, J.; Liu, G.; et al. High energy storage performance $MnSe_2$ cathode by one-step deposition strategy in aqueous zinc-ion batteries. *J. Alloys. Compd.* **2023**, *937*, 168424. DOI
128. Premkumar, M.; Vadivel, S.; Ramachandran, K.; Alshgari, R. A. Facile synthesis of novel $MnSe_2$/Ppy based cathode material for high capacity aqueous Zn-ion batteries. *J. Energy. Storage.* **2024**, *93*, 112210. DOI
129. Gao, X.; Shen, C.; Dong, H.; et al. Co-intercalation strategy for simultaneously boosting two-electron conversion and bulk stabilization of Mn-based cathodes in aqueous zinc-ion batteries. *Energy. Environ. Sci.* **2024**, *17*, 2287-97. DOI
130. Zhao, Z.; Ding, J.; Zhou, H.; Zhu, R.; Pang, H. Correction: concentration as a trigger to improve electrocatalytic activity of a Prussian blue analogue in glucose oxidation. *CrystEngComm* **2020**, *22*, 4190. DOI
131. Wang, Y.; Wang, Y.; Zhang, L.; Liu, C. S.; Pang, H. PBA@POM hybrids as efficient electrocatalysts for the oxygen evolution reaction. *Chem. Asian. J.* **2019**, *14*, 2790-5. DOI
132. Xu, D.; Wang, H.; Li, F.; et al. Conformal conducting polymer shells on V_2O_5 nanosheet arrays as a high-rate and stable zinc-ion battery cathode. *Adv. Mater. Inter.* **2019**, *6*, 1801506. DOI
133. Chen, L.; Yang, Z.; Cui, F.; Meng, J.; Chen, H.; Zeng, X. Enhanced rate and cycling performances of hollow V_2O_5 nanospheres for aqueous zinc ion battery cathode. *Appl. Surf. Sci.* **2020**, *507*, 145137. DOI
134. Bai, Y.; Zhang, H.; Xiang, B.; Yao, Q.; Dou, L.; Dong, G. Engineering porous structure in Bi-component-active ZnO quantum dots anchored vanadium nitride boosts reaction kinetics for zinc storage. *Nano. Energy.* **2021**, *89*, 106386. DOI
135. Park, J. S.; Wang, S. E.; Jung, D. S.; Lee, J. K.; Kang, Y. C. Nanoconfined vanadium nitride in 3D porous reduced graphene oxide microspheres as high-capacity cathode for aqueous zinc-ion batteries. *Chem. Eng. J.* **2022**, *446*, 137266. DOI
136. Lv, T.; Peng, Y.; Zhang, G.; et al. How about vanadium-based compounds as cathode materials for aqueous zinc ion batteries? *Adv. Sci.* **2023**, *10*, e2206907. DOI PubMed PMC
137. Rong, Y.; Chen, H.; Wu, J.; Yang, Z.; Deng, L.; Fu, Z. Granular vanadium nitride (VN) cathode for high-capacity and stable zinc-ion batteries. *Ind. Eng. Chem. Res.* **2021**, *60*, 8649-58. DOI
138. Zhang, Y.; Jiang, S.; Li, Y.; et al. In situ grown hierarchical electrospun nanofiber skeletons with embedded vanadium nitride nanograins for ultra-fast and super-long cycle life aqueous Zn-ion batteries. *Adv. Energy. Mater.* **2023**, *13*, 2202826. DOI
139. Yuan, Z.; Yang, X.; Lin, C.; et al. Progressive activation of porous vanadium nitride microspheres with intercalation-conversion reactions toward high performance over a wide temperature range for zinc-ion batteries. *J. Colloid. Interface. Sci.* **2023**, *640*, 487-97. DOI
140. Chen, X.; Wang, L.; Li, H.; Cheng, F.; Chen, J. Porous V_2O_5 nanofibers as cathode materials for rechargeable aqueous zinc-ion batteries. *J. Energy. Chem.* **2019**, *38*, 20-5. DOI
141. Hu, P.; Yan, M.; Zhu, T.; et al. Zn/V_2O_5 aqueous hybrid-ion battery with high voltage platform and long cycle life. *ACS. Appl. Mater. Interfaces.* **2017**, *9*, 42717-22. DOI
142. Li, J.; Mccoll, K.; Lu, X.; et al. Multi-scale investigations of δ-$Ni_{0.25}V_2O_5{\cdot}nH_2O$ cathode materials in aqueous zinc-ion batteries. *Adv. Energy. Mater.* **2020**, *10*, 2000058. DOI
143. Shin, J.; Choi, D. S.; Lee, H. J.; Jung, Y.; Choi, J. W. Hydrated intercalation for high-performance aqueous zinc ion batteries. *Adv. Energy. Mater.* **2019**, *9*, 1900083. DOI
144. Park, J. S.; Jo, J. H.; Aniskevich, Y.; et al. Open-structured vanadium dioxide as an intercalation host for Zn ions: investigation by first-principles calculation and experiments. *Chem. Mater.* **2018**, *30*, 6777-87. DOI
145. Chen, D.; Lu, M.; Wang, B.; et al. Uncover the mystery of high-performance aqueous zinc-ion batteries constructed by oxygen-doped vanadium nitride cathode: cationic conversion reaction works. *Energy. Storage. Mater.* **2021**, *35*, 679-86. DOI
146. Xu, X.; Ye, C.; Chao, D.; Davey, K.; Qiao, S. Z. Initiating Jahn-Teller effect in vanadium diselenide for high performance magnesium-based batteries operated at -40 °C. *Adv. Energy. Mater.* **2023**, *13*, 2204344. DOI

147. Bai, Y.; Zhang, H.; Xiang, B.; et al. Selenium defect boosted electrochemical performance of binder-free VSe_2 nanosheets for aqueous zinc-ion batteries. *ACS. Appl. Mater. Interfaces.* **2021**, *13*, 23230-8. DOI
148. Liu, Y.; Liu, Y.; Wu, X. Defect engineering of vanadium-based electrode materials for zinc ion battery. *Chin. Chem. Lett.* **2023**, *34*, 107839. DOI
149. Yang, J.; Yang, H.; Ye, C.; Li, T.; Chen, G.; Qiu, Y. Conformal surface-nanocoating strategy to boost high-performance film cathodes for flexible zinc-ion batteries as an amphibious soft robot. *Energy. Storage. Mater.* **2022**, *46*, 472-81. DOI
150. Liu, Y.; Liu, Y.; Wu, X.; Cho, Y. R. Enhanced electrochemical performance of Zn/VO_x batteries by a carbon-encapsulation strategy. *ACS. Appl. Mater. Interfaces.* **2022**, *14*, 11654-62. DOI
151. Cai, S.; Wu, Y.; Chen, H.; et al. Why does the capacity of vanadium selenide based aqueous zinc ion batteries continue to increase during long cycles? *J. Colloid. Interface. Sci.* **2022**, *615*, 30-7. DOI
152. Yang, M.; Wang, Y.; Ma, D.; et al. Unlocking the interfacial adsorption-intercalation pseudocapacitive storage limit to enabling all-climate, high energy/power density and durable Zn-ion batteries. *Angew. Chem. Int. Ed.* **2023**, *62*, e202304400. DOI
153. Qin, H.; Yang, Z.; Chen, L.; Chen, X.; Wang, L. A high-rate aqueous rechargeable zinc ion battery based on the VS_4@rGO nanocomposite. *J. Mater. Chem. A.* **2018**, *6*, 23757-65. DOI
154. He, P.; Yan, M.; Zhang, G.; et al. Layered VS_2 nanosheet-based aqueous Zn ion battery cathode. *Adv. Energy. Mater.* **2017**, *7*, 1601920. DOI
155. Jiao, T.; Yang, Q.; Wu, S.; et al. Binder-free hierarchical VS_2 electrodes for high-performance aqueous Zn ion batteries towards commercial level mass loading. *J. Mater. Chem. A.* **2019**, *7*, 16330-8. DOI
156. Pu, X.; Song, T.; Tang, L.; et al. Rose-like vanadium disulfide coated by hydrophilic hydroxyvanadium oxide with improved electrochemical performance as cathode material for aqueous zinc-ion batteries. *J. Power. Sources.* **2019**, *437*, 226917. DOI
157. Chen, T.; Zhu, X.; Chen, X.; et al. VS_2 nanosheets vertically grown on graphene as high-performance cathodes for aqueous zinc-ion batteries. *J. Power. Sources.* **2020**, *477*, 228652. DOI
158. Yin, B. S.; Zhang, S. W.; Xiong, T.; et al. Engineering sulphur vacancy in VS_2 as high performing zinc-ion batteries with high cyclic stability. *New. J. Chem.* **2020**, *44*, 15951-7. DOI
159. Yu, D.; Wei, Z.; Zhang, X.; et al. Boosting Zn^{2+} and NH_4^+ storage in aqueous media via in-situ electrochemical induced VS_2/VO_x heterostructures. *Adv. Funct. Mater.* **2021**, *31*, 2008743. DOI
160. Liu, J.; Peng, W.; Li, Y.; Zhang, F.; Fan, X. A VS_2@N-doped carbon hybrid with strong interfacial interaction for high-performance rechargeable aqueous Zn-ion batteries. *J. Mater. Chem. C.* **2021**, *9*, 6308-15. DOI
161. Zhu, J.; Jian, T.; Wu, Y.; et al. A highly stable aqueous Zn/VS_2 battery based on an intercalation reaction. *Appl. Surf. Sci.* **2021**, *544*, 148882. DOI
162. Yang, M.; Wang, Z.; Ben, H.; et al. Boosting the zinc ion storage capacity and cycling stability of interlayer-expanded vanadium disulfide through in-situ electrochemical oxidation strategy. *J. Colloid. Interface. Sci.* **2022**, *607*, 68-75. DOI
163. Samanta, P.; Ghosh, S.; Jang, W.; Yang, C.; Murmu, N. C.; Kuila, T. A reversible anodizing strategy in a hybrid electrolyte Zn-ion battery through structural modification of a vanadium sulfide cathode. *ACS. Appl. Energy. Mater.* **2021**, *4*, 10656-67. DOI
164. Chen, K.; Li, X.; Zang, J.; et al. Robust VS_4@rGO nanocomposite as a high-capacity and long-life cathode material for aqueous zinc-ion batteries. *Nanoscale* **2021**, *13*, 12370-8. DOI
165. Zhu, Q.; Xiao, Q.; Zhang, B.; et al. VS_4 with a chain crystal structure used as an intercalation cathode for aqueous Zn-ion batteries. *J. Mater. Chem. A.* **2020**, *8*, 10761-6. DOI
166. Liu, S.; Chen, X.; Zhang, Q.; Zhou, J.; Cai, Z.; Pan, A. Fabrication of an inexpensive hydrophilic bridge on a carbon substrate and loading vanadium sulfides for flexible aqueous zinc-ion batteries. *ACS. Appl. Mater. Interfaces.* **2019**, *11*, 36676-84. DOI
167. Han, J. H.; Lee, S.; Cheon, J. Synthesis and structural transformations of colloidal 2D layered metal chalcogenide nanocrystals. *Chem. Soc. Rev.* **2013**, *42*, 2581-91. DOI
168. Feng, J.; Peng, L.; Wu, C.; et al. Giant moisture responsiveness of VS_2 ultrathin nanosheets for novel touchless positioning interface. *Adv. Mater.* **2012**, *24*, 1969-74. DOI
169. Mai, L.; Wei, Q.; An, Q.; et al. Nanoscroll buffered hybrid nanostructural VO_2 (B) cathodes for high-rate and long-life lithium storage. *Adv. Mater.* **2013**, *25*, 2969-73. DOI
170. Bai, J.; Li, X.; Liu, G.; Qian, Y.; Xiong, S. Unusual formation of $ZnCo_2O_4$ 3D hierarchical twin microspheres as a high-rate and ultralong-life lithium-ion battery anode material. *Adv. Funct. Mater.* **2014**, *24*, 3012-20. DOI
171. Wang, T.; Gao, W.; Zhao, Y.; Wang, S.; Huang, W. Self-assembled VS_2 microflowers buffering volume change during charging and discharging towards high-performance zinc ion batteries. *J. Mater. Sci. Technol.* **2024**, *173*, 107-13. DOI
172. Zhu, Q.; Cheng, M.; Zhang, B.; et al. Realizing a rechargeable high-performance Cu-Zn battery by adjusting the solubility of Cu^{2+}. *Adv. Funct. Mater.* **2019**, *29*, 1905979. DOI
173. Schmidt, O.; Hawkes, A.; Gambhir, A.; Staffell, I. The future cost of electrical energy storage based on experience rates. *Nat. Energy.* **2017**, *2*, 2017110. DOI
174. Du, M.; Zhang, F.; Zhang, X.; et al. Calcium ion pinned vanadium oxide cathode for high-capacity and long-life aqueous rechargeable zinc-ion batteries. *Sci. China. Chem.* **2020**, *63*, 1767-76. DOI
175. Gao, X.; Liu, K.; Su, C.; et al. From bibliometric analysis: 3D printing design strategies and battery applications with a focus on zinc-ion batteries. *SmartMat* **2024**, *5*, e1197. DOI
176. Niu, F.; Bai, Z.; Chen, J.; et al. In situ molecular engineering strategy to construct hierarchical MoS_2 double-layer nanotubes for

ultralong lifespan “rocking-chair” aqueous zinc-ion batteries. *ACS. Nano.* **2024**, *18*, 6487-99. DOI

177. Lu, S. J.; Lin, J. Y.; Wang, C. H.; Zhang, Y. F.; Zhang, Y.; Fan, H. S. Heterogeneous engineering of MnSe@NC@ReS_2 core-shell nanowires for advanced sodium-/potassium-ion batteries. *Rare. Met.* **2024**, *43*, 3713-23. DOI